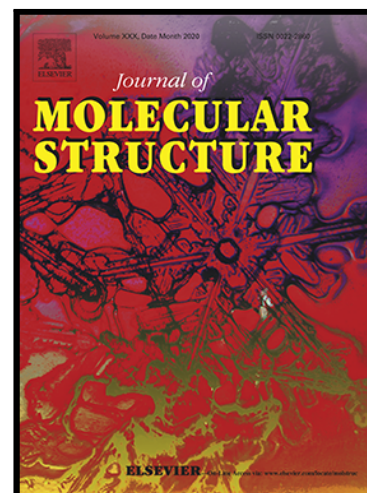


## Journal Pre-proof

Metal complexes derived from Hydrazoneoxime Ligands VI.  
Synthesis, characterization and structures of Zinc(II) complexes  
derived from aroylhydrazoneoximes

Nahed M H Salem , Sabine Foro , Magdi F. Iskander

PII: S0022-2860(20)31885-8  
DOI: <https://doi.org/10.1016/j.molstruc.2020.129571>  
Reference: MOLSTR 129571



To appear in: *Journal of Molecular Structure*

Received date: 22 July 2020  
Revised date: 2 October 2020  
Accepted date: 31 October 2020

Please cite this article as: Nahed M H Salem , Sabine Foro , Magdi F. Iskander , Metal complexes derived from Hydrazoneoxime Ligands VI. Synthesis, characterization and structures of Zinc(II) complexes derived from aroylhydrazoneoximes, *Journal of Molecular Structure* (2020), doi: <https://doi.org/10.1016/j.molstruc.2020.129571>

This is a PDF file of an article that has undergone enhancements after acceptance, such as the addition of a cover page and metadata, and formatting for readability, but it is not yet the definitive version of record. This version will undergo additional copyediting, typesetting and review before it is published in its final form, but we are providing this version to give early visibility of the article. Please note that, during the production process, errors may be discovered which could affect the content, and all legal disclaimers that apply to the journal pertain.

© 2020 Published by Elsevier B.V.

## Highlights

- Zn(II) complexes with diacetylmonoxime arylhydrazones were prepared.
- The molecular structure of the isolated complexes depends on the nature of substituents in the arylhydrazone ligands.
- Electron releasing substituents afforded dinuclear Zn(II) acetate complexes.
- Electron attracting substituents gave either mononuclear or linear polymeric chain Zn(II) acetate complexes.

Journal Pre-proof

**Metal complexes derived from Hydrazoneoxime Ligands VI. Synthesis,  
characterization and structures of Zinc(II) complexes derived from  
aroylhydrazoneoximes**

**Nahed M. H. Salem<sup>a</sup>, Sabine Foro<sup>b</sup>, Magdi F. Iskander<sup>\* a</sup>**

a) Chemistry Department, Faculty of Science, Alexandria University, P.O. box 426, Ibrahimia, Alexandria 21321, Egypt.

b) Material Science Department, Darmstadt Technical Univ., Alarich - Weiss str 4, 64287D Darmstadt, Germany.

Corresponding author: Prof. Dr. Magdi F. Iskander, E-mail < [m.iskander@link.net](mailto:m.iskander@link.net) >

E-mail address for Dr. Nahed M. H. Salem < [nahed\\_s@yahoo.com](mailto:nahed_s@yahoo.com) >

E-mail address for Sabine Foro < [foro@tu.darmstadt.de](mailto:foro@tu.darmstadt.de) >

**Abstract**

The reaction of  $Zn(OAc)_2 \cdot 2H_2O$  with substituted diacetylmonoxime aroylhydrazones  $H_2L-R$ ,  $R = H, p-CH_3, p-OCH_3, p-Cl$  and  $p-NO_2$ , using 1 : 1 molar ratio, in acidified ethanol as a solvent afforded  $[Zn(HL-H)(OAc)]_2 \cdot H_2O$  **1**,  $[Zn(HL-CH_3)(OAc)]_2 \cdot H_2O$  **2**,  $[Zn(HL-OCH_3)(OAc)]_2 \cdot H_2O$  **3**,  $[Zn(HL-Cl)(OAc)(H_2O)] \cdot H_2O$  **4**,  $[Zn(HL-NO_2)(OAc)]_3 \cdot n$  **5** respectively. The isolated complexes were characterized by elemental analysis, IR spectra, solution electronic absorption spectra, solution  $^1H$  NMR and  $^{13}C$  NMR spectra, and electrospray ionization mass spectra ESI-MS. The crystal and molecular structures of **1**, **2**, **4** and **5** have been determined by single crystal x-ray diffraction. Self assembly and supramolecular architectures of these complexes have been discussed. The substituent effects of the aroylhydrazone residue on the binding modes of acetate anion as well as the nuclearity and dimensionality of the formed complexes have been also discussed.

**Key Words**

Diacetylmonoxime aroylhydrazone, Zn(II) acetate complexes, Spectroscopy, X-ray crystal Structures.

## 1. Introduction

Multinuclear Zn(II) complexes have attracted attention for their structural diversity [1 – 14] together with their applications as photoluminescence [15 – 21], electroluminescence [22 – 23] and photoelectronic [24] materials. This class of Zn(II) complexes also finds application in the field of catalysis [25 – 27] and photocatalysis [28] and is also involved in the construction of metal – organic frameworks (MOFs) which can be used for gas adsorption and storage [29 – 31]. Accordingly, varieties of binuclear [1 – 3], trinuclear [3 – 5], tetranuclear [6 – 9] and polynuclear Zn(II) complexes [10 – 13] as well as Zn(II) polymers [14] have been synthesized and characterized.

Multinuclear Zn(II) complexes derived from aroylhydrazones have been also reported [1,6,28,32]. Aroylhydrazones ligands with appended potentially endogenous bridging groups can link Zn(II) ions in closed or open multinuclear clusters [6]. Multinuclear Zn(II) acetate aroylhydrazone complexes, where the acetate anion acts as bridging ligand have been synthesized and structurally characterized [1,6,32]. Introducing oxime moiety to the acyl/aroylhydrazone ligand e.g., diacetylmonoxime acyl/aroylhydrazones, resulted in the formation diprotic NNO tridentate ligands ( $H_2L$ ) [33]. Both monomeric neutral bisligand Zn(II) complexes  $[Zn(L)_2]$  [33,34] and mixed ligand Zn(II) acetate complexes having quinoline,  $[Zn(HL)(CH_3COO)(quin)] \cdot 0.5 \text{ quin}$  [35], and imidazole (HIm),  $[Zn(HL)(CH_3COO)(HIm)]$  [36], coligands have been structurally characterized. To the best of our knowledge, no multinuclear Zn(II) acetate complexes with diacetylmonoxime acyl/aroylhydrazones have been reported. These findings and in continuation to our studies on the coordination chemistry of Cu(II) and Ni(II) diacetylmonoxime acyl/aroylhydrazones [37 – 40] prompt our interest to study Zn(II) acetate complexes derived from diacetylmonoxime aroylhydrazones, aiming to clarify the effect of substituents of the

aroylhydrazone residue on the nuclearity and dimensionality of the obtained Zn(II) acetate complexes.

## 2. Experimental

### 2.1 Materials

Zn(II) acetate dihydrate was of reagent grade quality and was used as received without further purification. All solvents were distilled prior to use. Diacetylmonoxime was obtained from Acros and used without purification. Aroylhydrazines were prepared by hydrazinolysis of the corresponding methyl esters as previously described [41]. Aroylhydrazoneoxime ligands, H<sub>2</sub>L-R (R = H, CH<sub>3</sub>, CH<sub>3</sub>O, Cl and NO<sub>2</sub>), **Scheme 1**, were prepared by the condensation of diacetylmonoxime with the corresponding aroylhydrazine in methanol as previously described [40].

### 2.2 Synthesis of Zn(II) acetate complexes

To a solution of aroylhydrazonemonoxime, H<sub>2</sub>L-R (R = H, CH<sub>3</sub>, CH<sub>3</sub>O, Cl, NO<sub>2</sub>) (1.0 mmol) in ethanol (30 ml), a solution of zinc(II) acetate dihydrate (1.0 mmol, 0.2195 g) in ethanol (20 ml) was added. The resulting mixture was acidified with few drops of acetic acid and then heated with constant stirring for 1 hr. The solution was then allowed to stand undisturbed for few days until yellow crystals of the Zn(II) acetate complex were formed, then filtered off and dried, at room temperature, under vacuum.

2.2.1  $[Zn(HL-H)(OAc)]_2 \cdot H_2O$  **I**: Anal. Calc. for C<sub>26</sub>H<sub>32</sub>N<sub>6</sub>O<sub>9</sub>Zn<sub>2</sub>: C, 44.40; H, 4.59; N, 11.95. Found: C, 44.99; H, 4.89; N, 12.07%. IR(KBr) (cm<sup>-1</sup>): 3390 lattice water  $\nu(O-H)$ , 3155 hydrogen bonded oxime  $\nu(O-H)$ , 1610  $\nu(C=N-N=C)$ , 1580, 1628,  $\nu(OCO)_{asym.}$ , 1535  $\nu(C=N)_{ox}$ , 1468, 1385  $\nu(OCO)_{sym.}$ , 1030  $\nu(N-O)$ . UV-Vis (EtOH,  $\lambda_{max}/nm$  (log $\epsilon$ ): 240 (4.30), 350 (4.43), 380 sh. <sup>1</sup>H NMR (DMSO-d<sub>6</sub>, ppm): 1.92 (6H, CH<sub>3</sub>COO), 2.09, 2.14 (6H, CH<sub>3</sub>-C=NOH), 2.36, 2.37 (6H, CH<sub>3</sub>-C=NN), 7.42 (6H, aromatic), 8.11, 8.12 (4H, aromatic),

10.73 (2H, H<sub>2</sub>O), 11.73, 13.52 (2H, oxime O–H). <sup>13</sup>C{<sup>1</sup>H} NMR (DMSO-d<sub>6</sub>, ppm): 10.57, 11.38 (CH<sub>3</sub>-C=N-OH), 13.50, 13.77 (CH<sub>3</sub>-C=NN), 22.90 (CH<sub>3</sub>COO), 127.51, 127.68, 127.87, 129.78, 130.47, 136.18, 136.98 (CH-aromatic), 147.34, 148.23 (C=N-OH), 149.96, 150.91 (C=NN), 171.84, 172.61 (C<sub>6</sub>H<sub>5</sub>-CO), 176.58 (CH<sub>3</sub>COO). (+)ESI – MS (DMF/CH<sub>3</sub>OH) m/z Calcd. (RA): 216.1 (216.5290) (1.5) [Zn(OAc)<sub>2</sub>(CH<sub>3</sub>OH)]; 256.7 (257.5813) (2.0) [Zn(OAc)<sub>2</sub>(DMF) + H<sup>+</sup>]<sup>1+</sup>; 283.1 (283.6247) (14.2) [Zn(HL-H)]<sup>1+</sup>; 343.5 (343.6771) (3.7) [Zn((HL-H)(OAc) + H<sup>+</sup>)]<sup>1+</sup>; 355.8 (356.7191) (14.5) [Zn(HL-H)(DMF)]<sup>1+</sup>; 417.5 (416.7715) (3.7) [Zn(HL-H)(OAc)(DMF) + H<sup>+</sup>]<sup>1+</sup>; 429.6 (429.8136) (2.5) [Zn(HL-H)(DMF)<sub>2</sub>]<sup>1+</sup>; 501.1 (502.8673) (17.2) [Zn(HL-H)<sub>2</sub> + H]<sup>1+</sup>; 583.1 (584.2567) (33.6) [{Zn(L-H)}<sub>2</sub>(H<sub>2</sub>O) + H]<sup>1+</sup>; 625.1(626.2939) (37.3) [{Zn(HL-H)<sub>2</sub>(OAc)]<sup>1+</sup>; 638.2 (639.3359) (100) [{Zn(L-H)}<sub>2</sub>(DMF) + H]<sup>1+</sup>; 711.2 (712.4304) (34.3) [{Zn(L-H)}<sub>2</sub>(DMF)<sub>2</sub> + H]<sup>1+</sup>; 761.7 (759.4408) (7.6) [{Zn(HL-H)(OAc)}<sub>2</sub>(DMF) + H]<sup>1+</sup>; 848.2 (848.8584) (42.3) [{Zn(L-H)}<sub>3</sub> + H]<sup>1+</sup>; 921.2 (921.9527) (25.6) [{Zn(L-H)<sub>3</sub>(DMF) + H]<sup>1+</sup>; 1129.1 (1131.4751) (35.8) [{Zn(L-H)}<sub>4</sub> + H]<sup>1+</sup>.

2.2.2 [*Zn(HL-CH<sub>3</sub>)(OAc)*]<sub>2</sub>·H<sub>2</sub>O 2: Anal. Calc. for C<sub>28</sub>H<sub>36</sub>N<sub>6</sub>O<sub>9</sub>Zn<sub>2</sub>: C, 45.98; H, 4.96; N, 11.49. Found: C, 46.55; H, 5.17; N, 11.34%. IR(KBr) (cm<sup>-1</sup>): 3390 lattice water ν(O–H), 3160 oxime ν(O–H), 1630, 1580 ν(OCO)<sub>asym.</sub>, 1612 ν(C=N–N=C), 1530 ν(C=N)<sub>ox</sub>, 1460, 1380 ν(OCO)<sub>sym.</sub>, 1025 ν(N–O). UV–Vis (EtOH, λ<sub>max</sub>/nm (logε): 252(4.26), 357 (4.42), 388 sh. <sup>1</sup>H NMR (DMSO-d<sub>6</sub>, ppm): 1.93 (6H, CH<sub>3</sub>COO), 2.05, 2.12 (6H, CH<sub>3</sub>–C=NOH), 2.36 (6H p-CH<sub>3</sub>-C<sub>6</sub>H<sub>4</sub>), 2.36, 2.38 (6H, CH<sub>3</sub>–C=NN), 7.20, 7.22 (4H, aromatic), 8.01, 8.02 (4H, aromatic), 11.60, 13.36, (2H, oxime O–H). <sup>13</sup>C{<sup>1</sup>H} NMR (DMSO-d<sub>6</sub>, ppm): 10.59, 11.31 (CH<sub>3</sub>-C=NOH), 13.45, 13.74 (CH<sub>3</sub>-C=NN), 18.51, 21.02 (p-CH<sub>3</sub>C<sub>6</sub>H<sub>4</sub>), 23.15 (CH<sub>3</sub>COO), 127.56, 127.77, 128.29, 128.50, 133.45, 134.20, 139.32, 140.30 (CH-aromatic), 147.34, 148.23 (C=NOH), 149.45, 150.00 (C=NN), 170.10, 172.50 (C<sub>6</sub>H<sub>5</sub>-CO), 177.19 (CH<sub>3</sub>COO). (+) ESI – MS (DMF/CH<sub>3</sub>OH) m/z Calcd. (RA): 257.2 (257.5813) (3.70) [Zn(OAc)<sub>2</sub>(DMF) +

$H^+$ ]; 329.0 (329.6935) (1.7)  $[Zn(HL-CH_3)(CH_3OH)]^{1+}$ ; 357.2 (357.7039) (2.0)  $[Zn(HL-CH_3)(OAc) + H^+]$ ; 369.2 (370.7459) (10.3)  $[Zn(HL-CH_3)(DMF)]^{1+}$ ; 430.2 (430.7983) (2.0)  $[Zn(HL-CH_3)(DMF) + H^+]^{1+}$ ; 443.2 (443.8404) (5.0)  $[Zn(HL-CH_3)(DMF)_2]^{1+}$ ; 503 (503.8927) (8.0)  $[Zn(HL-CH_3)(OAc)(DMF)_2 + H^+]$ ; 529.3 (530.9210) (10.3)  $[Zn(HL-CH_3)_2 + H^+]$ ; 594.2 (594.2952) (36.8)  $[Zn(L-CH_3)]_2 + H^+$ ; 612.2 (612.3104) (25.3)  $[Zn(L-CH_3)]_2(H_2O) + H^+$ ; 654.2 (654.3476) (13.2)  $[Zn(HL-CH_3)]_2(OAc)^{1+}$ ; 668.2 (667.3896) (100.0)  $[Zn(L-CH_3)]_2(DMF) + H^+$ ; 740.53 (740.4840) (20.7)  $[Zn(L-CH_3)]_2(DMF)_2 + H^+$ ; 787.2 (787.4943) (8.8)  $[Zn(HL-CH_3)(OAc)]_2(DMF) + H^+$ ; 890.2 (890.9387) (19.2)  $[Zn(L-CH_3)]_3 + H^+$ ; 963.3 (964.0331) (34.1)  $[Zn(L-CH_3)]_3(DMF) + H^+$ ; 1187.2 (1187.5824) (48.8)  $[Zn(L-CH_3)]_4 + H^+$ ; 1298.4 (1298.7671) (35.8).

**2.2.3  $[Zn(HL-CH_3O)(OAc)]_2 \cdot H_2O$  3:** Anal. Calc. for  $C_{28}H_{36}N_6O_{11}Zn_2$ : C, 44.06; H, 4.75; N, 11.00. Found: C, 44.87; H, 4.73; N, 10.39%. IR(KBr) ( $cm^{-1}$ ): 3400 lattice water  $\nu(O-H)$ , 3158 oxime  $\nu(O-H)$ , 1628, 1585  $\nu(OCO)_{asym.}$ , 1610  $\nu(C=N-N=C)$ , 1530  $\nu(C=N)_{ox}$ , 1470, 1387  $\nu(OCO)_{sym.}$ , 1028  $\nu(N-O)$ . UV-Vis (EtOH,  $\lambda_{max}/nm$  ( $\log \epsilon$ ): 265 (4.21), 360 (4.47), 395 sh.  $^1H$  NMR (DMSO- $d_6$ , ppm): 1.900, (6H,  $CH_3COO$ ), 1.973, 2.125 (6H,  $\underline{CH_3-C=NOH}$ ), 2.338, 2.351 (6H,  $\underline{CH_3-C=NN}$ ), 3.814 (6H,  $OCH_3$ ), 6.957, 6.971, 6.977 (4H, aromatic), 8.047, 8.064 (4H, aromatic), 10.65, (2H, O-H), 11.75, 13.36 (2H, oxime O-H).  $^{13}C$  { $^1H$ } NMR (DMSO- $d_6$ , ppm): 10.59, 11.33 ( $\underline{CH_3-C=N-OH}$ ), 13.38, 13.68 ( $\underline{CH_3-C=NN}$ ), 22.53 ( $\underline{CH_3COO}$ ), 56.02 ( $p-\underline{CH_3OC_6H_4}$ ), 112.96, 113.21, 129.14, 129.46 (CH-aromatic), 147.55, 148.20 ( $\underline{C=N-OH}$ ), 149.45, 150.00 ( $\underline{C=NN}$ ), 170.10, 172.51 ( $C_6H_5-\underline{CO}$ ), 175.76 ( $\underline{CH_3COO}$ ). (+) ESI - MS (DMF/ $CH_3OH$ )  $m/z$  Calcd. (RA): 216.2 (216.5290) (6.0)  $[Zn(OAc)_2(CH_3OH) + H^+]^{1+}$ ; 248 (248.5710) (2.0)  $[Zn(OAc)_2(CH_3OH)_2 + H^+]^{1+}$ ; 257.3 (257.5813) (1.6)  $[Zn(OAc)_2(DMF) + H^+]^{1+}$ ; 312.7 (313.6510) (4.8)  $[Zn(HL-OCH_3)]^{1+}$ ; 330.2 (330.6757) (6.0)  $[Zn(OAc)_2(DMF)_2 + H^+]^{1+}$ ; 372.5 (373.7034) (6.0)  $[Zn(HL-CH_3O)(OAc) +$

$\text{H}]^{1+}$ ; 386.2 (386.7453)  $[\text{Zn}(\text{HL-CH}_3\text{O})(\text{DMF})]^{1+}$ ; 446.2 (446.7977) (2.0)  $[\text{Zn}(\text{HL-CH}_3\text{O})(\text{OAc})(\text{DMF}) + \text{H}^+]^{1+}$ ; 459.2 (459.8397) (4.8)  $[\text{Zn}(\text{HL-CH}_3\text{O})(\text{DMF})_2]^{1+}$ ; 519.5 (519.8920) (4.5)  $[\text{Zn}(\text{HL-CH}_3\text{O})(\text{OAc})(\text{DMF})_2 + \text{H}^+]^{1+}$ ; 645.1 (644.3104) (100)  $[\{\text{Zn}(\text{L-CH}_3\text{O})\}_2 + (\text{H}_2\text{O}) + \text{H}^+]^{1+}$ ; 685.1 (686.3464) (6.2)  $[\{\text{Zn}(\text{HL-CH}_3\text{O})\}_2(\text{OAc})]^{1+}$ ; 698.2 (699.3883) (20.8)  $[\{\text{Zn}(\text{L-CH}_3\text{O})\}_2(\text{DMF}) + \text{H}^+]^{1+}$ ; 772.2 (772.4828) (11.5)  $[\{\text{Zn}(\text{L-CH}_3\text{O})\}_2(\text{DMF})_2 + \text{H}^+]^{1+}$ ; 769.0 (769.3886) (10.4)  $[\{\text{Zn}(\text{HL-CH}_3\text{O})(\text{OAc})\}_2 + \text{Na}]^{1+}$ ; 938.1 (938.9370) (38.1)  $[\{\text{Zn}(\text{L-CH}_3\text{O})\}_3 + \text{H}^+]^{1+}$ ; 1251.1 (1251.5799) (19.4)  $[\{\text{Zn}(\text{L-CH}_3\text{O})\}_4 + \text{H}^+]^{1+}$ .

**2.2.4  $[\text{Zn}(\text{HL-Cl})(\text{OAc})(\text{H}_2\text{O})].2\text{H}_2\text{O}$  4:** Anal. Calc. for  $\text{C}_{13}\text{H}_{20}\text{ClN}_3\text{O}_7\text{Zn}$ : C, 36.22; H, 4.66; N, 9.75. Found: C, 36.77; H, 4.630; N, 9.905%. IR (KBr) ( $\text{cm}^{-1}$ ): 3388 coordinated water  $\nu(\text{O}-\text{H})$ , 3137 oxime  $\nu(\text{O}-\text{H})$ , 1659  $\nu(\text{OCO})_{\text{asym.}}$ , 1620  $\nu(\text{C}=\text{N}-\text{N}=\text{C})$ , 1520  $\nu(\text{C}=\text{N})_{\text{ox}}$ , 1426  $\nu(\text{OCO})_{\text{sym}}$ , 1035  $\nu(\text{N}-\text{O})$ . UV-Vis (EtOH,  $\lambda_{\text{max}}/\text{nm}$  ( $\log \epsilon$ ): 248 (4.01), 355 (4.10), 400 sh;  $^1\text{H}$  NMR (DMSO- $d_6$ , ppm): 1.91 (3H,  $\text{CH}_3\text{COO}$ ), 2.09 (3H,  $\text{CH}_3-\text{C}=\text{NN}$ ), 2.32 (3H,  $\text{CH}_3-\text{C}=\text{NOH}$ ), 7.43, 7.44 (2H, aromatic), 8.06, 8.07 (2H, aromatic), 10.74 (2H, Coordinated  $\text{H}_2\text{O}$ ), 13.42 (1H, oxime  $\text{O}-\text{H}$ ).  $^{13}\text{C}\{^1\text{H}\}$  NMR (DMSO- $d_6$ , ppm): 11.92 ( $\underline{\text{C}}\text{H}_3-\text{C}=\text{N}-\text{OH}$ ), 14.23 ( $\underline{\text{C}}\text{H}_3-\text{C}=\text{NN}$ ), 23.48 ( $\underline{\text{C}}\text{H}_3\text{COO}$ ), 128.37, 128.58, 129.83, 130.04, 135.60 (CH-aromatic), 148.86 ( $\underline{\text{C}}=\text{N}-\text{OH}$ ), 151.26 ( $\underline{\text{C}}=\text{NN}$ ), 172.82 ( $\text{C}_6\text{H}_5-\underline{\text{C}}\text{O}$ ), 177.20 ( $\text{CH}_3\underline{\text{C}}\text{OO}$ ). (+) ESI – MS (DMF/ $\text{CH}_3\text{OH}$ )  $m/z$  Calcd. (RA): 216.2 (216.5290) (2.0)  $[\text{Zn}(\text{OAc})_2(\text{CH}_3\text{OH}) + \text{H}^+]^{1+}$ ; 248 (248.5710) (1.0)  $[\text{Zn}(\text{OAc})_2(\text{CH}_3\text{OH})_2 + \text{H}^+]^{1+}$ ; 257.3 (257.5813) (1.5)  $[\text{Zn}(\text{OAc})_2(\text{DMF}) + \text{H}^+]^{1+}$ ; 318.0 (318.0699) (12.0)  $[\text{Zn}(\text{HL-Cl})]^{1+}$ ; 330 (330.6757) (2.0)  $[\text{Zn}(\text{OAc})_2(\text{DMF})_2 + \text{H}^+]^{1+}$ ; 350.2 (350.1119) (10.0)  $[\text{Zn}(\text{OAc})(\text{CH}_3\text{OH})]^{1+}$ ; 378.2 (378.1223) (10.0)  $[\text{Zn}(\text{HL-Cl})(\text{OAc}) + \text{H}^+]^{1+}$ ; 391.0 (391.1642) (6.0)  $[\text{Zn}(\text{HL-Cl})(\text{DMF})]^{1+}$ ; 451.0 (451.2166) (3.0)  $[\text{Zn}(\text{HL-Cl})(\text{OAc})(\text{DMF}) + \text{H}^+]^{1+}$ ; 464.2 (464.2587) (3.7)  $[\text{Zn}(\text{HL-Cl})(\text{DMF})_2]^{1+}$ ; 524.0 (524.3109) (2.0)  $[\text{Zn}(\text{HL-Cl})(\text{DMF})_2 + \text{H}^+]^{1+}$ ; 653.2 (653.1469) (75.5)  $[\{\text{Zn}(\text{L-Cl})\}_2(\text{H}_2\text{O}) + \text{H}^+]^{1+}$ ; 695.2 (695.1842) (8.0)  $[\{\text{Zn}(\text{HL-Cl})\}_2(\text{OAc})]^{1+}$ ; 708.0 (708.2261)

(8.5) [ $\{Zn(L-Cl)\}_2(DMF) + H^+$ ] $^{1+}$ ; 781.2 (781.3206) (12.5) [ $\{Zn(L-Cl)\}_2(DMF)_2 + H^+$ ]; 952.0 (952.1936) (100) [ $\{ZnL-Cl\}_3 + H^+$ ] $^{1+}$ ; 1025.0 (1025.2880) (5.0) [ $\{Zn(L-Cl)\}_3(DMF) + H^+$ ] $^{1+}$ ; 1269.0 (1269.2556) (7.5) [ $\{Zn(L-Cl)\}_4 + H^+$ ] $^{1+}$ .

2.2.5  $[Zn(HL-NO_2)(OAc)]_3$  **5**: Anal. Calc. for  $C_{13}H_{14}N_4O_6Zn$ : C, 40.28; H, 3.64; N, 14.45. Found: C, 40.65; H, 3.69; N, 14.40%. IR(KBr) ( $cm^{-1}$ ): 3170  $\nu(O-H)$ , 1620  $\nu(C=N-N=C)$ , 1560  $\nu(OCO)_{asym.}$ , 1527  $\nu(C=N)_{ox}$ , 1440  $\nu(OCO)_{sym.}$ , 1023  $\nu(N-O)$ . UV-Vis (EtOH,  $\lambda_{max}/nm$  ( $\log \epsilon$ ): 263 (4.40). 385 (4.39), 410 sh;  $^1H$  NMR (DMSO- $d_6$ , ppm): 1.92 (3H,  $CH_3COO$ ), 2.13, 2.15 (3H,  $CH_3-C=NOH$ ), 2.39, 2.41(3H,  $CH_3-C=NN$ ), 8.28, 8.29 (2H, aromatic), 8.33, 8.35 (2H, aromatic), 13.60 (H, oxime O-H).  $^{13}C\{^1H\}$  NMR (DMSO- $d_6$ , ppm): 10.55, 11.37 ( $\underline{C}H_3-C=N-OH$ ), 13.66, 13.94 ( $\underline{C}H_3-C=NN$ ), 22.59 ( $\underline{C}H_3COO$ ), 123.06, 123.19, 128.54, 128.68, 128.78 (CH-aromatic), 148.58 ( $\underline{C}=N-OH$ ), 152.27 ( $\underline{C}=NN$ ), 170.59 ( $C_6H_5-\underline{C}O$ ), 177.50 ( $CH_3\underline{C}OO$ ). (+) ESI MS (DMF/ $CH_3OH$ ) m/z Calcd. (RA): 216.2 (216.5290) (2.5) [ $Zn(OAc)_2(CH_3OH) + H^+$ ] $^{1+}$ ; 248.1 (248.5710) (2.5) [ $Zn(OAc)_2(CH_3OH)_2 + H^+$ ] $^{1+}$ ; 257.2 (257.5813) (3.5) [ $Zn(OAc)_2(DMF) + H^+$ ] $^{1+}$ ; 328.0 (328.6223) (7.5) [ $Zn(HL-NO_2)]^{1+}$ ; 330.0 (330.6757) (3.8) [ $Zn(OAc)_2(DMF)_2 + H^+$ ] $^{1+}$ ; 360.2 (360.6644) (8.2) [ $Zn(HL-NO_2)(CH_3OH)]^{1+}$ ; 388.0 (388.6747) (8.5) [ $Zn(HL-NO_2)(OAc) + H^+$ ] $^{1+}$ ; 401.2 (401.7168) (5.2) [ $Zn(HL-NO_2)(DMF)]^{1+}$ ; 461.0 (461.7692) (2.0) [ $Zn(HL-NO_2)(DMF) + H^+$ ] $^{1+}$ ; 474.2 (474.8111) (2.0) [ $Zn(HL-NO_2)(DMF)_2 + H^+$ ] $^{1+}$ ; 534.0 (534.8635) (3.5) [ $Zn(HL-NO_2)(OAc)_2 + H^+$ ] $^{1+}$ ; 674.0 (674.2520) (60.8) [ $\{Zn(L-NO_2)\}_2(H_2O)+H^+$ ] $^{1+}$ ; 729.0 (729.3311) (9.5) [ $\{Zn(L-NO_2)\}_2(DMF) + H^+$ ] $^{1+}$ ; 802.0 (802.4256) (15.0) [ $\{Zn(L-NO_2)\}_2(DMF)_2 + H^+$ ] $^{1+}$ ; 983.2 (983.8511) (100) [ $\{Zn(L-NO_2)\}_3 + H^+$ ] $^{1+}$ ; 1056.0 (1056.9456) (4.5) [ $\{Zn(L-NO_2)\}_3(DMF) + H^+$ ] $^{1+}$ ; 1311.0 (1311.4655) (6.0) [ $\{Zn(L-NO_2)\}_4 + H^+$ ] $^{1+}$ .

### 2.3 Physical measurement

Elemental analyses (C, H, N) were performed at the Micro analytical Laboratory, at Institut für Organische Chemie Technische Universität, Darmstadt, Germany. The infrared spectra

were recorded on a Perkin-Elmer 1430 Data system and/or a Perkin-Elmer (FT-IR) Paragon 1000 PC spectrophotometer. Solid samples were examined as KBr discs. The UV-Vis absorption spectra were recorded on V-530 Jasco, recording spectrophotometer, using 10 mm quartz cells.  $^1\text{H}$  NMR and  $^{13}\text{C}$  NMR spectra were recorded on Bruker WM 300 and/or JEOL 500 MHz spectrometer using tetramethylsilane (TMS) as an internal standard. ESI mass spectra were recorded on Esquire-LC from Bruker Daltonic Nebulizer 10psi (dry gas,  $8\text{Lmin}^{-1}$ , dry temperature  $250\text{ }^\circ\text{C}$ ). X-ray diffraction data for  $[\text{Zn}(\text{HL-H})(\text{OAc})]_2\cdot\text{H}_2\text{O}$  **1** and  $[\text{Zn}(\text{HL-CH}_3)(\text{OAc})]_2\cdot\text{H}_2\text{O}$  **2** complexes were collected on a Nonius CADY diffractometer, while diffraction data for  $[\text{Zn}(\text{HL-Cl})(\text{OAc})(\text{H}_2\text{O})]_2\cdot 2\text{H}_2\text{O}$  **4** and  $[\text{Zn}(\text{HL-NO}_2)(\text{OAc})]_n$  **5**, complexes were collected on Oxford Diffraction Xcalibur (TM) single crystal X-ray diffractometer with Sapphire CCD detector. Graphite monochromated Mo  $\text{K}\alpha$  radiation ( $\lambda = 0.71013\text{ \AA}$ ) was used in all cases. The structures were solved by direct methods with SHELXS-97 [42] and refined with full-matrix least squares on F2 using SHELXL-97 [42]. Hydrogens were positioned with idealized geometry using a riding model and were refined with isotropic displacement parameter. Drawings of the molecules were produced with ORTEP3 [43] or PLATON [44]. Parameters of hydrogen bonds, and other non-covalent bond interactions were measured using PLATON [44] and MERCURY (CCDC) [45]. Crystal data and details concerning data collection and structure refinements for  $[\text{Zn}(\text{HL-H})(\text{OAc})]_2\cdot\text{H}_2\text{O}$  **1**,  $[\text{Zn}(\text{HL-CH}_3)(\text{OAc})]_2\cdot\text{H}_2\text{O}$  **2**,  $[\text{Zn}(\text{HL-Cl})(\text{OAc})(\text{H}_2\text{O})]_2\cdot 2\text{H}_2\text{O}$  **4**, and  $[\text{Zn}(\text{HL-NO}_2)(\text{OAc})]_n$  **5**, are given in **Table 1**.

### 3. Results and Discussion

#### 3.1 Synthesis and stoichiometry

The reaction of  $\text{Zn}(\text{OAc})_2\cdot 2\text{H}_2\text{O}$  with aroylhydrazoneoximes having electron donating substituents ( $\text{H}_2\text{L-R}$ ,  $\text{R} = \text{H}$ ,  $p\text{-CH}_3$  and  $p\text{-OCH}_3$ ) in acidified ethanol using (1 : 1 molar ratio)

afforded the dinuclear Zn(II) complexes  $[\{Zn(HL-R)(OAc)\}_2] \cdot H_2O$  **1** – **3**. However, on using aroylhydrazoneoximes with electron withdrawing substituents ( $H_2L-R$ ,  $R = Cl$  and  $NO_2$ ), the reaction proceeded with the formation of mononuclear  $[Zn(HL-Cl)(OAc)(H_2O)] \cdot 2H_2O$  (**4**) and trinuclear  $[\{Zn(HL-NO_2)(OAc)\}_3]$  (**5**).

### 3.2 Infrared Spectra

The IR spectra of Zn(II) acetate complexes **1** – **5**, lack absorptions due to  $\nu(N-H)$ , amide I [ $\nu(C=O)$ ] and amide II vibrations, but show intense absorption within the range  $1610 - 1620 \text{ cm}^{-1}$  due to  $\nu(C=N-N=C)$  of the deprotonated aroylhydrazone residue [46,47]. The spectra also show absorptions at  $3130 - 3170$ ,  $1520 - 1535$  and  $1020 - 1030 \text{ cm}^{-1}$ , respectively, due to hydrogen bonded oxime  $\nu(O-H)$ ,  $\nu(C=N)_{ox}$  and  $\nu(N-O)$  of the hydroxyimino residue. These absorption bands are shifted to lower frequencies relative to those of the free ligands. The recorded spectral patterns indicate the deprotonation of the enolimine form of the aroylhydrazone residue while the oxime residue remains protonated [37 – 40]. The aroylhydrazoneoxime ligand in these complexes acts as monoanionic NNO tridentate ligand, coordinating to Zn(II) *via* azomethine hydrazone nitrogen, deprotonated enolimine oxygen and oxime nitrogen [37 – 40].

The acetate anion in Zn(II) acetate complexes, generally, has versatile coordination behavior, it can act as monodentate, chelating, bidentate bridging, monoatomic bridging and chelating bridging ligands [48, 52]. The magnitude of the separation between the asymmetric and symmetric carboxylate stretches,  $\Delta\nu = \nu_{as}(OCO) - \nu_s(OCO)$ , is frequently used as a diagnostic parameter for carboxylate binding mode in metal(II) complexes [53 – 58]. The IR spectra of the dinuclear **1**, **2** and **3** complexes display strong absorptions within the range  $1628 - 1630 \text{ cm}^{-1}$  due to acetate  $\nu_{as}(OCO)$  vibration, while the corresponding  $\nu_s(OCO)$  vibrations appear within the range  $1460 - 1470 \text{ cm}^{-1}$ . The average frequency separation  $\Delta\nu$

between  $\nu_{\text{as}}(\text{OCO})$  and  $\nu_{\text{s}}(\text{OCO})$  is  $163 \text{ cm}^{-1}$ , suggesting *syn-syn* bidentate bridging ( $\mu_2-\eta^1:\eta^1$ ) mode [50,53]. The spectra also show absorptions at  $1580 - 1585 \text{ cm}^{-1}$  and  $1380 - 1387 \text{ cm}^{-1}$  due to  $\nu_{\text{as}}(\text{OCO})$  and  $\nu_{\text{s}}(\text{OCO})$  respectively. The average value of  $\Delta\nu = 198 \text{ cm}^{-1}$  is in accordance with monoatomic bridging acetate ( $\mu_2-\eta^2:\eta^0$ ) coordination mode [55,58]. Both monodentate and *syn-syn* bidentate bridging modes assigned for the acetate anions in **1** and **2** have been confirmed by X-ray structural analysis (section 3.5). The IR spectrum of the mononuclear **4** complex displays the acetate  $\nu_{\text{as}}(\text{COO})$  and  $\nu_{\text{s}}(\text{COO})$  vibrations respectively at  $1659$  and  $1426 \text{ cm}^{-1}$  with frequency separation ( $\Delta\nu = 233 \text{ cm}^{-1}$ ) significantly higher than that reported for ionic acetate ( $140 - 164 \text{ cm}^{-1}$ ), indicating monodentate coordination mode ( $\mu_1-\eta^1:\eta^0$ ) [55, 58]. This coordination mode has been also confirmed by X-ray molecular structure (section 3.5). The  $\nu_{\text{as}}(\text{COO})$  and  $\nu_{\text{s}}(\text{COO})$  acetate vibrations in the spectrum of **5** complex appear respectively at  $1560$  and  $1440 \text{ cm}^{-1}$ . The observed low value of  $\Delta\nu$  ( $120 \text{ cm}^{-1}$ ) relative to that of sodium acetate suggests *syn-anti* bidentate bridging coordination mode ( $\mu_2-\eta^1:\eta^1$ ) [49,51,52,58] which is also confirmed by X-ray molecular structure (section 3.5).

Both of the stoichiometry and IR spectral data of Zn(II) acetate complexes **1-5** reveal that the nuclearity and acetate coordination modes of these complexes are mainly influenced by the nature of the substituent in the aroylhydrazone residue of the aroylhydrazoneoxime ligand. Electron donating substituents in the dinuclear **1-3** complexes tend to increase the formal negative charge (*i.e.* increase in basicity) of the deprotonated enolimine oxygen of the aroylhydrazone residue and hence decrease the formal positive charge (*i.e.* decrease in Lewis acidity) of the Zn(II) centers. This will favor the formation of the dinuclear structure where the two Zn(II) centers are linked together by *syn-syn* bidentate and monoatomic bridging acetate anions. On the other hand, electron withdrawing substituents (*p*-chloro and *p*-nitro) in the aroylhydrazone residue resulted in a relative increase of the formal positive charge on Zn(II). This leads to the formation of neutral mononuclear complex **4** where terminal

monodentate acetate anion is coordinated to the Zn(II) atom. To minimize the repulsion between Zn(II) centers in polymeric complex **5**, the successive Zn(II) centers are connected together by *syn* – *anti* acetate bridges rather than *syn* – *syn* or monoatomic acetate bridges.

### 3.3 UV – Vis Absorption Spectra

The solution (UV – VIS) absorption spectra of the free aroylhydrazoneoxime ligands H<sub>2</sub>L-R (R = H, p-CH<sub>3</sub>, p-OCH<sub>3</sub>, p-Cl, and p-NO<sub>3</sub>) (**Scheme 1**) in ethanol have been previously reported [38 – 40]. The spectra display two intense absorptions, respectively, at (230, 267 nm), (235, 278 nm), (244, 285 nm), (234, 280 nm) and (253, 295 nm) due to  $\pi \cdots \pi^*$  transitions. These absorption bands show red shift in the corresponding spectra of Zn(II) acetate complexes **1** – **5** and appear at (240, 350 nm), (252, 357 nm), (265, 360 nm), (248, 355 nm) and (263, 285 nm) respectively. The spectra also show a new absorption, as a shoulder, within the range (380 – 410 nm) due to MLCT transition [1, 6]. The observed spectral changes, as compared to the spectra of free ligands, can be tentatively attributed to the coordination of Zn(II) to H<sub>2</sub>L-R ligands which resulted in the deprotonation of the enolimine tautomer and consequently form two  $\pi$ -delocalized 5,5-membered chelate rings. This will extend conjugation along the ligand frame and resulted in a decrease of the energy gap between n and  $\pi^*$  orbitals. In the spectra of Zn(II) complexes **1** – **5**, the absorptions due to both  $\pi - \pi^*$  and MLCT transitions depend on the nature of substituent in the terminal phenyl group of the aroylhydrazone residue. The variation of the maximum absorption, expressed in wave number (cm<sup>-1</sup>), as a function of Hammett substitution parameter ( $\sigma$ ), **Figure 1**; suggests two different excited states related to two different chromophores. The lower excited state involves the aroylhydrazone chromophore (**Scheme 2-a**) where the negative charge is localized on the deprotonated oxygen of the enolimine tautomer while the positive charge is localized on the phenyl end. The higher excited state involves the diimine-oxime

chromophore (**Scheme 2-b**) where the positive charge is localized on the protonated oxygen of the nitroso tautomer while the negative charge is localized on the phenyl end.

### 3.4 $^1\text{H}$ NMR and $^{13}\text{C}$ NMR Spectra

The solution  $^1\text{H}$  NMR spectra of the dinuclear Zn(II) acetate complexes **1** – **3** in DMSO- $d_6$  display a pair of singlets at 2.08 – 2.14 ppm corresponding to the two methyl groups adjacent to the oxime residue ( $\text{CH}_3\text{C}=\text{NOH}$ ), while the two methyl groups adjacent to the aroylhydrazone residue ( $\text{CH}_3\text{C}=\text{NN}$ ) are more deshielded and appear as two singlets at 2.34 – 2.40 ppm. This behavior is in agreement with asymmetric dinuclear structure where the two coordinated aroylhydrazoneoxime ligands are situated in different environments. Similarly, the spectrum of the trinuclear  $[\{\text{Zn}(\text{HL-NO}_2)(\text{OAc})\}_3]$  **5** also displays two singlets for each of ( $\text{CH}_3\text{C}=\text{NOH}$ ) (2.13, 2.15 ppm) and ( $\text{CH}_3\text{C}=\text{NN}$ ) (2.39, 2.41 ppm) methyl protons suggesting that in this trinuclear molecular unit, each of these methyl groups is situated in two different orientations. The spectrum of the mononuclear  $[\text{Zn}(\text{HL-Cl})(\text{OAc})(\text{H}_2\text{O})].2\text{H}_2\text{O}$  **4** shows singlets at 2.09 and 2.321 ppm, respectively due to ( $\text{CH}_3\text{C}=\text{NOH}$ ) and ( $\text{CH}_3\text{C}=\text{NN}$ ) methyl protons indicating mononuclear structure. Furthermore, the spectra of Zn(II) acetate complexes **1** – **5** lack any signal that can be attributed to hydrazinic NH proton indicating the deprotonation of the enolimine form of the aroylhydrazone residue. The spectra, however, display broad signals within the range 11.33 – 11.75 and 13.36 – 13.56 ppm respectively due to intermolecular and intramolecular hydrogen bonded oxime  $=\text{NOH}$  proton.

The solution  $^{13}\text{C}$  NMR spectra of **1** – **3**, in DMSO- $d_6$ , also show pairs of resonances at 10.50 – 11.6 and 13.5 – 14.45 ppm, respectively due to ( $\underline{\text{C}}\text{H}_3\text{C}=\text{NOH}$ ) and ( $\underline{\text{C}}\text{H}_3\text{C}=\text{NN}$ ) methyl carbon nuclei. At lower field, the spectra also display pairs of resonances within the range 142.40 – 150.90, 147.30 – 152.27 and 169.09 – 172.77 ppm, respectively due  $\text{C}=\text{NOH}$ ,  $\text{C}=\text{NN}$  and Ar.CO carbon nuclei. The spectrum of **4** however, show peaks at 11.92, 14.23,

148.86, 151.26 and 172.82 ppm, respectively attributed to  $\text{CH}_3=\text{NOH}$ ,  $\text{CH}_3\text{C}=\text{NN}$ ,  $\text{C}=\text{NOH}$ ,  $\text{C}=\text{NN}$  and  $\text{Ar.CO}$  carbon nuclei of the coordinated ligand. Here again the presence of only one singlet for each of the carbon nuclei of the coordinated hydrazoneoxime ligands in the  $^{13}\text{C}$  NMR spectra of **4** is in agreement with mononuclear structure.

The  $^1\text{H}$  NMR spectra of the dinuclear  $\text{Zn(II)}$  acetate complexes **1** – **3** display one singlet at 1.90 – 1.93 ppm for the acetate  $\text{CH}_3$  protons. The  $^{13}\text{C}$  NMR spectra also show two resonances at 22.53 – 23.15 and 175.76 – 177.19 ppm respectively due to acetate  $\text{CH}_3$  and  $\text{OC(O)}$  carbon nuclei. Both  $^1\text{H}$  NMR and  $^{13}\text{C}$  NMR spectra indicate that at ambient temperature the bidentate bridging and monodentate bridging acetates in **1** – **3** complexes are indistinguishable. This can be ascribed to a rapid reversible interconversion of the monoatomic bridging acetate to syn-syn bidentate bridging acetate (carboxylate shift) at a rate faster than NMR time scale [59]. This facile interconversion is due to the labile nature of the spherical  $d^{10}$  configuration of  $\text{Zn(II)}$  [60] as well as the extremely fluxional acetate coordination in these dinuclear complexes. The monoatomic bridging acetate plays a crucial role in this carboxylate shift process [59]. The dangling oxygen of this monoatomic bridging acetate initially interacts with  $\text{Zn1}$  leading to a labile intermediate or transition state **C**, **Scheme 3**, where  $\text{O1}$  and  $\text{O2}$  of monoatomic bridging acetate as well as  $\text{O3}$  and  $\text{O4}$  of bidentate bridging acetate are linked respectively to  $\text{Zn1}$  and  $\text{Zn2}$  through semicoordinate bonds. Simultaneous coordination of  $\text{O1}$  to  $\text{Zn1}$  and  $\text{O3}$  to  $\text{Zn2}$  followed by rotation around  $\text{O3} - \text{C}$  bond resulted in the transformation of monoatomic to bidentate bridging acetate as shown in **Scheme 3**. Furthermore, the  $^1\text{H}$  NMR spectrum of **4** displays one singlet at 1.91 due to acetate  $\text{CH}_3$  protons. The  $^{13}\text{C}$  NMR spectrum also show one singlet at 23.5 for  $\text{CH}_3$  carbon in addition to another singlet at 177.20 ppm due to  $\text{OC(O)}$  carbon. The recorded spectra suggest a mononuclear structure where the  $\text{Zn(II)}$  is, most probably coordinated to terminal monodentate acetate.

### 3.5 ESI- Mass Spectra.

The (+) ESI-mass spectra of Zn(II) complexes **1** – **3** display peaks, of very low (RA) values, corresponding to dinuclear  $[\{Zn(HL-R)(OAc)\}_2 + H^+]^{1+}$  and mononuclear  $[Zn(HL-R)(OAc) + H^+]^{1+}$  (R = H, CH<sub>3</sub>, and CH<sub>3</sub>O) species, while **4** and **5** complexes show only weak peaks due to the mononuclear species  $[Zn(HL-R)(OAc) + H^+]^{1+}$  (R = Cl and NO<sub>2</sub>), suggesting extensive dissociation. The spectra of **1** – **5** complexes also show peaks corresponding to  $[Zn(HL-R)(DMF)_n + H^+]^{1+}$  and  $[Zn(OAc)(DMF)_n + H^+]^{1+}$  (n = 0, 1 or 2) generated, respectively, from the expulsion of OAc<sup>-</sup> and HL-R<sup>-</sup> anions, from  $[Zn(HL-R)(OAc)(DMF)_n + H^+]^{1+}$ . Deprotonation of the oxime group of the coordinated ligand, during electrospray ionization leads to the formation of the mononuclear oximate  $[Zn(L-R)(DMF)_n]^{1+}$  cation followed by stepwise association reactions, through oximate bridge, giving rise to di-, tri- and tetranuclear cations as shown in **Scheme 4**. This behavior has been previously reported for Ni(II) and Cu(II) complexes derived from diacetylmonoxime acyl/aroylhydrazone complexes [37 – 40].

### 3.5 Molecular Structures and Supramolecular Architectures

The x-ray crystal structures of **1**, **2**, **4** and **5** complexes reveal that the central Zn(II) in these complexes is situated in a distorted square pyramidal environment. This is evident from the calculated values of the tetragonality parameters,  $\tau = [(\beta - \alpha) / 60]$  [61], given in **Table 2**. Bond distances and bond angles of the Zn(II) polyhedrons for **1**, **2**, **4** and **5** are listed, respectively, in **Tables ( S1 – S4)**. The x-ray structure of  $[\{Zn(HL-H)(OAc)\}_2].H_2O$  (**1**), **Figure 2**, consists of dinuclear Zn(II) molecular unit and one solvate water molecule. Each of Zn1 and Zn2 is coordinated to the mononegative NNO tridentate hydrazone oxime anion (HL-H)<sup>-</sup> via oxime nitrogen (Zn1 – N3 = 2.177(10), Zn2 – N6 = 2.236(10) Å), imine nitrogen (Zn1 – N1 = 2.003(10), Zn2 – N4 = 1.991(10) Å) and deprotonated enolimine

oxygen (Zn1 – O2 = 2.110(7), Zn2 – O6 = 2.058(8) Å), forming 5,5- bicyclic chelate ring. The Zn1(HL-H) and Zn2(HL-H) moieties are linked together through the monoatomic bridging acetate O1 oxygen (Zn1 – O1 = 1.974(8), Zn2 – O1 = 1.951(8) Å) and O4 and O5 oxygen atoms of the *syn – syn* bidentate bridging acetate (Zn1 – O4 = 1.935(10), Zn2 – O5 = 2.003(9) Å). The basal planes of Zn1 and Zn2 are defined, respectively, by oxime (N3 and N6) nitrogen, imine (N1 and N4) nitrogen and deprotonated enolimine (O2 and O6) oxygen of the mononegative tridentate hydrazonoxime ligand. The fourth coordination site of both Zn1 and Zn2 are occupied by the monoatomic bridging acetate O1 oxygen. The fifth apical coordination sites for Zn1 and Zn2 are occupied, respectively, by O4 and O5 of the bidentate bridging acetate oxygen's. The Zn1 is separated from Zn2 by 3.257 Å and both Zn1 and Zn2 are, respectively, displaced from the corresponding basal plane by 0.500 and 0.416 Å towards the apical bidentate acetate O4 and O5 oxygen.

The solvate water molecules in the crystal lattice of **1** play a crucial role in the process of self assembly. Each two solvate water molecules act as bridges joining two binuclear Zn(II) molecular units through reciprocal pairs of (O9H91...O8, H91...O8 = 1.987(9) Å) hydrogen bonds (HB's) between water H91 proton and uncoordinated monoatomic bridging O8 oxygen, (O9H92...O6, H92...O6 = 2.021(9) Å) HB's between water H92 and the deprotonated enolimine O6 oxygen and (O9...H3O, O9...H3 = 1.873 Å) HB's between water O9 oxygen and oxime H3O proton, giving rise to supramolecular tetranuclear assembly. These units are further linked together by reciprocal pairs of (C24H24C... $\pi_1$ , H24C...Cg1 = 2.887 Å), **Table S5**, between methyl C24H24C proton of the bidentate acetate and the delocalized  $\pi$  system of the metalloaromatic chelate ring (N1, N2, C1.O2, Zn1) [62], giving rise to <sup>1</sup>D chain of supramolecular tetranuclear units propagating along *a*-axis (**Figure 3-a**). The chains are further joined together via CH... $\pi$  interactions between methyl C23H23A

proton and aromatic ring (C12 – C17)  $\pi$ -system (C23H23a $\cdots\pi_2$ , C23H23a $\cdots$ Cg2 = 3.009 Å) generating 2D layer extended parallel to crystallographic *ac*- plane (**Figure 3-b**). The layers are further interconnected by pairs of CH $\cdots$ O, (C14H14 $\cdots$ O8, C14H14 $\cdots$ O8 = 2.641 Å) HB's forming <sup>3</sup>D framework which is stabilized by (C23H23c $\cdots\pi_3$ , H23c $\cdots$ Cg3 = 2.720 Å) and (C7H7 $\cdots\pi_3$ , C7H7 $\cdots$ Cg3 = 3.662 Å) CH $\cdots\pi$  interactions (**Table S5**).

Similar to **1**, the x-ray structure of [ $\{Zn(HL-CH_3)(OAc)\}_2$ ].H<sub>2</sub>O (**2**), **Figure 4**, consists of dinuclear molecular units where each of Zn1 and Zn2 is, respectively, coordinated to the mononegative NNO tridentate hydrazoneoxime anion (HL-CH<sub>3</sub>)<sup>-1</sup> via oxime nitrogen (Zn1 – N1 = 2.186(2), Zn2 – N4 = 2.2284(19) Å), imine nitrogen (Zn1 – N2 = 2.021(2), Zn2 – N5 = 2.0177(19) Å) and deprotonated enolimine oxygen (Zn1 – O1 = 2.1057(16), Zn2 – O6 = 2.8828 (17)). The Zn1 and Zn2 are also coordinated to O4 and O5 oxygen atoms of the bidentate bridging acetate, in addition to O3 of the monodentate bridging acetate (Zn1 $\cdots$ O3 = Zn2 $\cdots$ O3 = 1.9980 (16)). Both Zn1 and Zn2 are displaced from the corresponding basal planes (N1, N2, O1, O3) and (N4, N5, O6, O3) towards the bidentate bridging acetate oxygen atoms O4 and O5 by 0.381 Å and 0.479 Å, respectively. The distance between Zn1 and Zn2 (Zn1 $\cdots$ Zn2 = 3.376 Å) is relatively longer than that recorded for complex **1**. This can be attributed to the electron releasing effect of the p-CH<sub>3</sub>- substituent of this dinuclear complex. The dinuclear molecular units are linked together via CH $\cdots$ O hydrogen bonds (C10H10c $\cdots$ O4, C10H10 $\cdots$ O4 = 2.511 Å) and (C12H12b $\cdots\pi_1$ , C12H12b $\cdots$ Cg1 = 2.899 Å) CH $\cdots\pi$  interactions, Table **S6**, giving rise to a helical chain running along c-axis (c-chain) (**Figure 5-a**). The c-chains are associated together through solvent water bridges via (O9H91 $\cdots$ N6, O91 $\cdots$ N6 = 2.136(4) Å) hydrogen bond (HB) between water H91 proton and hydrazidic N6 nitrogen, (O9H92 $\cdots$ O6, H92 $\cdots$ O6 = 2.322(5) Å) HB between water H92 proton and deprotonated enolimine O6, in addition to (O2H2 $\cdots$ O9,

$O2H2\cdots O9 = 1.849(4)$  Å) between oxime H2 proton and water O9 forming 2D layer extended parallel to bc-plane (bc layer). The layer structure is further stabilized by ( $C28H28A\cdots O6$ ,  $H28A\cdots O8 = 2.665$  Å) HB between methyl C28H28 proton and enolimine O6 oxygen as shown in **Figure 5-b**. Two ac-layers are interconnected through ( $C14H14c\cdots O8$ ,  $C14cH14\cdots O8 = 2,878$  Å) and ( $C24H24\cdots O8$ ,  $C24H24\cdots O8 = 2.624$  Å) HB's generating 2D double layered structure.

Different from the structures of **1** and **2**, where the Zn(II) acetate complexes exist as dinuclear molecular units, the x-ray structure of **4**, **Figure 6**, consists of mononuclear molecular unit  $[Zn(HL-Cl)(OAc)(H_2O)]$  and two solvate water molecules. The basal plane of **4** is defined by oxime N3 nitrogen ( $Zn1 - N3 = 2.144$  Å), imine N2 nitrogen ( $Zn1 - N2 = 2.057$  Å), enoleimine O1 oxygen ( $Zn - O1 = 2.080$  Å), and monodentate acetate O2 oxygen ( $Zn1 - O2 = 1.962$  Å). The coordinated water O5 oxygen is situated in the fifth apical coordination site ( $Zn1 - O5 = 2.001$  Å). The Zn1 is displaced from the basal plane (N3, N2, O1, O2) towards acetate O5 oxygen by 0.431 Å. The coordinated water H51 proton and the monodentate acetate O3 oxygen are involved in the formation of reciprocal pairs of  $CH\cdots O$  hydrogen bonds ( $O5H51\cdots O3$ ,  $H51\cdots O3 = 1.867$  Å) giving rise to head to tail supramolecular dimeric unit. These dimeric units are associated together through two solvent water bridges *via* reciprocal pairs of ( $O7H71\cdots O2$ ,  $H71\cdots O2 = 2.100$  Å) Hydrogen bonds, between water H71 proton and monodentate acetate O2 oxygen and ( $O7H72\cdots N1$ ,  $H72\cdots N1 = 2.192$  Å) HB between water H72 proton and hydrazidic N2 nitrogen, leading to the formation of 1D chain running along c-axis (c-chain) (**Figure 7**). The c-chains are linked together through ( $O6H61\cdots O1$ ,  $H61\cdots O1 = 2.099$  Å), ( $O6H62\cdots O7$ ,  $H62\cdots O7 = 2.012$  Å), ( $O5H52\cdots O6$ ,  $H52\cdots O6 = 1.896$  Å) and ( $C6H6\cdots O5$ ,  $H6\cdots O5 = 2.632$  Å)  $CH\cdots O$  hydrogen bonds, generating to 2D layer of dimeric units extended parallel to ac plane. The layers are further

interconnected through (C4H4 $\cdots$ O7, C4 $\cdots$ O7 = 3.465 Å), (C12H12A $\cdots$ O6, C12 $\cdots$ O6 = 3.623 Å) and (C13H13C $\cdots$ O4, C13 $\cdots$ O4 = 3.448 Å) CH $\cdots$ O hydrogen bonds, forming <sup>3</sup>D framework, through which rectangular channels are running parallel to *b*-axis.

The x-ray crystal structure of [ $\text{Zn}(\text{HL-NO}_2)(\text{OAc})_3$ ] **5**, **Figure 8**, consists of trinuclear [ $\text{Zn}(\text{HL-NO}_2)(\text{OAc})_3$ ] molecular units which are linked together through syn - anti bidentate bridged acetate anions, forming helical polymeric chain running parallel to *b*-axis. The bond distances and bond angles of Zn1 polyhedron are listed in **Table S4**. The oxime N1 nitrogen, imine N2 nitrogen and enolimine O1 oxygen of the coordinated hydrazone oxime ligand in addition to the bidentate bridged acetate O2 oxygen constitute the basal plane, while the bridged acetate O3 oxygen of the adjacent molecular unit occupies the fifth apical site. The Zn1 is displaced from the basal plane (N1, N2, O1, O2), towards the apical O3 oxygen, by 0.54 Å. The polymeric helical chain is stabilized by pairs of hydrogen bonds between O4H4 oxime proton and O2 (O4H4 $\cdots$ O2, O4 $\cdots$ O2 = 3.071 Å) and O3 (O4H4 $\cdots$ O3, O4 $\cdots$ O3 = 2.751 Å) oxygen atoms of the syn - anti bidentate bridging acetate. The helical chains are linked together via pairs of reciprocal hydrogen bonds between the O6 oxygen of the nitro group and C12H12A methyl proton (C12H12A $\cdots$ O6, C12 $\cdots$ O6 = 3.443 Å) and C3H3 aromatic proton (C3H3 $\cdots$ O6, C3 $\cdots$ O6 = 3.287 Å), **Table S8**, giving a layer of helical chains extended parallel to *bc*- plane. The layers are further connected to each other through (C11H11C $\cdots$ O5, C11 $\cdots$ O5 = 3.411 Å) hydrogen bond between the acetate methyl C11H11C proton and nitro group O5 oxygen, in addition to CH $\cdots$  $\pi$  interaction between methyl C13H13A proton and C2 - C7 aromatic ring  $\pi$  - system (C13H13A $\cdots$ Cg1 = 3.085 Å), **Table S8**, forming <sup>3</sup>D framework structure.

### 3.6 Conclusion

The reaction of  $\text{Zn}(\text{OAc})_2 \cdot 2\text{H}_2\text{O}$  with substituted diacetylmonoxime aroylhydrazones ( $\text{H}_2\text{L-R}$ ) ( $\text{R} = \text{H}, \text{p-CH}_3, \text{p-OCH}_3, \text{p-Cl}$  and  $\text{p-NO}_2$ ), using (1 : 1) molar ratio, in acidified ethanol as a solvent afforded  $[\{\text{Zn}(\text{HL-H})(\text{OAc})\}_2] \cdot \text{H}_2\text{O}$  **1**,  $[\{\text{Zn}(\text{HL-CH}_3)(\text{OAc})\}_2] \cdot \text{H}_2\text{O}$  **2**,  $[\{\text{Zn}(\text{HL-OCH}_3)(\text{OAc})\}_2] \cdot \text{H}_2\text{O}$  **3**,  $[\text{Zn}(\text{HL-Cl})(\text{OAc})(\text{H}_2\text{O})] \cdot 2\text{H}_2\text{O}$  **4**,  $[\{\text{Zn}(\text{HL-NO}_2)(\text{OAc})\}_3]_n$  **5** respectively. Both nuclearity and acetate coordination modes in **1 – 5** complexes are affected by the nature of the substituent in the terminal phenyl group of the hydrazide moiety. Electron donating substituent ( $\text{R} = \text{H}, \text{CH}_3, \text{OCH}_3$ ) in **1 – 3** complexes tend to decrease the formal positive charge of  $\text{Zn}(\text{II})$  and favor the formation of dinuclear complexes. In **1 – 3** complexes, the  $\text{Zn}(\text{II})$  atoms are linked together by *syn – syn* and monoatomic bridging acetate anions. Electron withdrawing substituents ( $\text{R} = \text{Cl}$  and  $\text{NO}_2$ ) in **4** and **5** complexes resulted in an increase of the formal positive charge of  $\text{Zn}(\text{II})$ . To avoid repulsion between  $\text{Zn}(\text{II})$  atoms mononuclear  $\text{Zn}(\text{II})$  acetate complex **4** as well as linear chain polymer **5** were obtained. In **4** the terminal acetate acts as monodentate anion, while in **5** the  $\text{Zn}(\text{II})$  atoms are linked together by *syn – anti* bridging acetate anions.

The electronic absorption spectra of  $\text{Zn}(\text{II})$  acetate complexes **1 – 5** reveal that both electron donating or electron withdrawing substituents in the hydrazide residue resulted in a red shift for both  $\pi - \pi^*$  and MLCT absorption bands. This behavior suggests two different excited states originated from the excitation of keto/enol aroylhydrazone moiety and oxime/protonated nitroso chromophores.

## Supplementary data

CCDC 1985722, 1985613, 1985620, 1985619 contain the supplementary crystallographic data for 1, 2, 4 and 5 complexes, respectively. These data can be obtained free of charge via <http://www.ccdc.cam.ac.uk/conts/retrieving.html>, or from Cambridge crystallographic Data center, 12 Union Road Cambridge CB2 IEZ, UK (fax: +44-1223-336033; e-Mail: [deposit@ccdc.ac.uk](mailto:deposit@ccdc.ac.uk) or www: <http://www.ccdc.cam.ac.uk>).

## Supplementary material

Contains Tables for bond distances, bond angles and structural parameters of non covalent bond interactions for 1, 2, 4, 5 complexes

## ACKNOWLEDGEMENT

Dr. Nahed M. H. Sallem would like to thank Faculty of Science, Alexandria University for supporting the present work through "Science Research Enhancement Program (Science REP) 2011.

## Author statement

Nahed Salem, carried out all the experimental work, collect the experimental results and writing the experimental section; Sabina foro , solved the x-ray crystal structures and collecting the x-ray structural data; M. Iskander , discuss and interpret the data, writing and editing the text including all art work.

## Conflict of interest

The authors declare that they have no known competing financial interests or personal relationship that could have appeared to influence the work reported in this paper.

## References

- [ 1 ] G. Xu, B. -B. Tang, L. Hao, G. -L. Liu, H. Li, CrystEngComm. 19 (2017) 781.
- [ 2 ] S. Roy, B. N. Sakar, K. Bhar, S. Satapathi, P. Mitra, B. Ghosh, J. Mol. Struct. 1037 (2013) 160.
- [ 3 ] G. Guethol, P. Sobota, Acta Cryst. C69 (2013) 372.
- [ 4 ] O. Q. Monro, K. Gillham, M. P. Akerman, Acta Cryst. , C65 (2009) m317.

- [ 5 ] S. Lin, M. -X. Yang, S. -X Liu, *Polyhedron*, 26 (2007) 4793.
- [ 6 ] B. -B. Tang, H. Ma, G. -Z. Li, Y. -B. Wang, G. Anwar, R. Shi, H. Li, *CrystEngComm.*, 15, (2013) 8069.
- [ 7 ] A. Patra, T. K. Sen, R. Bhattacharyya, S. K. Mandal, M. Bera, *RCS advances*, 2 (2012) 1774.
- [ 8 ] G. Marinescu, A. M. Madalan, S. Shova, M. Andruh, *J. Coord. Chem.*, 65 (2012) 1539.
- [ 9 ] S. -C. Chen, R. -M. Yu, Z. -G. Zhao, S. -M. Chen, Q. -S. Zhang, X. -Y. Wu, F. Wang, C. -Z Lu, *Cryst. Growth Des.*, 10 (2010) 1155.
- [10] S. Akine, W. Dong, T. Nabeshima, *Inorg. Chem.*, 45 (2006) 4677.
- [11] A. Cingolani, S. Galli, N. Masciocchi, L. Pandolfo, C. Pettinari, A. Sironi, *Dalton Trans.*, (2006) 2479.
- [12] F. A. Alkami, A. A. Khandar, G. Mahmoud, M. Amini, E. Molins, P. Garczarek, J. Lipkowski, J. M. White, A. M. Kiriuov, *Inorg. Chim. Acta*, 356 (2006) 2246.
- [13] A. Waheed, R. A. Jones, J. McCarty and X. Yang, *Dalton Trans.*, (2004) 3840.
- [14] A. Erxleben, *Coord. Chem. Rev.* 246 (2003) 203.
- [15] X. -Y. Dong, L. Gao, F. Wang, Y. Zhang, W. -K. Dong, *Crystals*, 7 (2017) 267.
- [16] F. Borbone, U. C. Concillio, S. Nabha, B. Panunzi, S. P. R. Shinkler, A. Tuzi, *Eur. J. Inorg. Chem.* 818 (2016) 818.
- [17] G. -C. Xu, L. Zhang, Y. H. Zhang, J. X. Guo, *CystEngComm.* 15 (2013) 2873.
- [18] C. Z. Lu, *cryst. Growth Des.* 10 (2010) 1155.
- [19] Y. O. Fan, X. K. Huo, L. Wang, L. F. Ma, *J. Coord. Chem.* 60 (2007) 1619.
- [20] S. -L. Zheng, X. -M. Chen, *Aust. J. Chem.* 57 (2004) 703.
- [21] S. Mizukami, H. Houjou, K. Sugaya, E. Koyama, H. Tokuhisa, T. Sasaki, M. Kanetsato, *Chem. Mat.*, 17 (2005) 50.
- [22] R. Wang, L. Deng, M. Fu, J. Cheng, J. Li, *J. Mater Chem.* 22 (2012) 23454.
- [23] P. Wang, Z. Hung, Z. Xie, S. Tong, O. Wong, C. -S. Lee, N. Wong, L. Hung, S. Lee, *Chem. Commun.*, (2003) 1664.
- [24] W. LiPing, Jiao ShiBo, Zhang WeiFeng, Liu Yun Qi, Yu Gui, *Chinese Science Bulletin*, 58 (2013) 2733.
- [25] J. Xia, Y. Xu, S. -an Li, W. -Y. Sun, K. -B. Yu, W. -X Tang, *Inorg. Chem.* 40 (2001) 2394.
- [26] L. Bonfa, M. Gatos, F. Mucin, P. Tecilla, U. Tonellato, *Inorg. Chem.*, 42 (2003) 3943.
- [27] J. xia, Y. Xu, S. -A. Li, W. -Y. Sun, K. -B. Yu, W. X. Tang, *Inorg. Chem.* 40 (2001) 2394.

- [28] Y. Wu, J. He, S. Wang, L. Zou, X. Wu, *Inorg. Chim. Acta*, 458 (2017) 218.
- [29] J. L. C. Rowsel, O. M. Yaghi, *Angew. Chem. Int. Ed.* 44 (2005) 4670.
- [30] H. Chun, D. N. Dyntsev, H. Kim and O. M. Yaghi, *J. Amer. Chem. Soc.* 128 (2006).
- [31] T. Ohshima, T. Iwasaki, K. Mashima, *Chem. Commun.*, (2006) 2711.
- [32] X. –H. Peng, X. –L. Tang, W. –W. Quin, W. Dou, Y. –L. Guo, J. –R. Zheng, W. –S. Wang, *Dalton Trans.*, 40 (2011) 5271.
- [33] S. Naskar, D. Mishra, R. J. Butcher, S. K. Chattopadhyay, *Polyhedron*, 26 (2007) 3703.
- [34] M. Mahmmod Al-Ne'aimi, M. M. Al – Khuder, *Spectrochim. Acta*, A105 (2013) 365.
- [35] S. Gao, L. –H. Huo, J. –W. Liu, C. Wang, J. –G. Zhao, S. –W. Ng, *Acta Cryst* , E 60 (2004) m. 644 – m 646.
- [36] L. –H. Huo, S. Gao, J. –W. Liu, C. Wang, J. –G. Zhao, *Acta Cryst.* 60 (2004) m.696 – m 646.
- [37] N. M. H. Salem , L. El - Sayed , W. Haase, M. F. Iskander, *Spectrochimica Acta Part A*, 134 (2015) 257.
- [38] N. M. H. Salem, L. El-Sayed, S. Fro, W. Haase, M. F. Iskander *Polyhedron*, 26 (2007) 416.
- [39] N. M. H. Salem, L. El- Sayed, W. Haase, M. F. Iskander, *J. Coord. Chem.*, 58, (2005) 1327.
- [40] M. F. Iskander, L. El-Sayed, N. M. H. Salem, R. Werner, W. Haase, *J. Coord. Chem.* 56 (2003) 1075.
- [41] M. F. Iskander, S. E. Zayan, M. A. Khalifa, L. El Sayed, *J. Inorg. Nucl. Chem.*, 36 (1974) 551.
- [42] G. M. Sheldrich, *SHELXI-97: Program for Crystal structure Analysis*, University of Gottingen, Gottingen, 1998.
- [43] C. K. Johnson, M. N. Burnett, *ORTEPIII*, Report ORNL-6895, Oak Ridge National Laboratory, TN, USA, 1996.
- [44] A. L. Spek, *PLATON, A Multipurpose Crystallographic Tool*, Utrecht University, Utrecht, The Netherlands, 2002.
- [45] C. F. Macrae, I. J. Bruno, J. A. Chishoim, P. R. Eddington, P. McCabe, E. Pidcocke, L. Rodriguez-Monge, R. Taylor, J. Vande Streek, P. A. Wood, *J. Appl. Crystallogr.* 41 (2008) 466.
- [46] M. F. Iskander, L. El-Sayed, M. A. Lasheen, *Inorg. Chim. Acta*, 16 (1976) 147.
- [47] L. El-Sayed, M. F. Iskander, *J. inorg. nucl. Chem.*, 33 (1971) 435.
- [48] U. Kumar, J. Thomas, N. Thirupathi, *Inorg. Chem.*, 49 (2010) 62.
- [49] V. Zelenak, I. Cisarova, P. Llewellyn, *Inorg. Chem. Commun.* 10, (2007) 27.

- [50] C. R. Choudhury, A. Datta, V. Gromlich, G. M. G. Hossain, K. M. Abdul Malik, S. Mitra, *Inorg.Chem. Commun.*, 10 (2007) 27.
- [51] W. Clegg, V. Buchholz, V. Enkelmann, B. B. Snider, B. M. Foxman, *Chem. Comm.* 42 (2000) 2225.
- [52] W.Clegg, D. R. Harborn, D. C. Homan, P. A. Hunt, I. R. Little, B. P. Straughan, *Inog. Chem. Acta*, 186 (1991) 51.
- [53] Z. Vargova, M. Almasi, L. Arabuli, K. Gyoryova, V. Zelenak, J. Kuchar, *Spectrochim. Acta*, A78 (2011).
- [54] D. Martinez, M. Motevali, M. Watkinson, *Dalton Trans.* , 39 (2010) 446.
- [55] V. Zelenak, Z. Vargova, K. Gyoryova, *Spectrochim. Acta*, A66 (2007) 262.
- [56] D. Martini, M. Pellei, C. Pettinari, B. W. Skeleton, A. H. White, *Inorg. Chim. Acta*, 333 (2002) 72.
- [57] T. Ishioka, Y. Shibata, M. Takahashi, I. Kanesaka, Y. Kitakawa, K. T. Nakamura, *Spectrochim. Acta*, A54 (1998) 1827.
- [58] G. B. Deacon and R. J. Phillips, *Coord. Chem. Rev.* 33 (1980).
- [59] A. Demsar, J. Kosmrlj, S. Petricek, J. Arner. *Chem. Soc.* 124 (2002) 3951.
- [60] D. E. Wilcox, *Chem. Rev.* 96 (1996) 2435.
- [61] A. W. Addison, T. Nageswara Roa, J. Reedjik, J. Van Rijin, G. C. Verschoor, *J. Chem. Soc. Dalton Trans.* (1984) 1349.
- [62] H. Masui, *Coord. Chem. Rev.* 219 (2001) 957.

### List of changes and rebuttals

- 1) The title of the paper has been diminished.
- 2) Parentheses between the numbers of complexes have been deleted.
- 3) Polynuclear or multinuclear complexes, in this article, are coordination compounds containing two or more metal atoms or ions in single coordination sphere. The metallic centers are bounded together through metal – metal bonds , bridging ligands or ligands substituted with substituents having donor atoms which can coordinate with one or more metallic centers. Polymeric metal complex or coordination polymer is a coordination complex between polymeric matrix consists of a chain of monomeric bi-, tri or multidentate ligand capable to bound one or more metallic ion forming polymeric linear or helical chain. Polymeric Chains of di-, tri...or metallic cluster can be also considered as coordination polymers.
- 4) Information concerning multinuclear Zn(II) acetate acyl/arylhydrazones as well as diacetylmonoxime acyl/arylhydrazones complexes have been introduced in the Introduction section.
- 5) Only four parts (I, II, III and V) (ref. 37 – 40) of this series of ( coordination chemistry of hydrazoneoxime ligands) are concerned with the coordination chemistry Cu(II) and Ni(II) complexes with diacetylmonoxime acyl/arylhydrazones. Part IV deals with complexes derived from diacetylmonoxime S-benzylhydrazinedithiocarboxylate. The new aspects of the present article (part VI) are given at the end of introduction section.
- 6) In the experimental section, H<sub>2</sub>L-R (1,R....)1, is meaningless and has been omitted .
- 7) <sup>1</sup>HNMR and <sup>13</sup>CNMR have been corrected.
- 8) The rapid interconversion from monodentate to bidentate acetate ligands in solution, given in the text, is based on NMR studies at room temperature. However, the reaction mechanism given in **Scheme 3** is a well established mechanism based on dynamic NMR studies at different temperature (ref. 59) and not speculative. This part is very important to understand and appreciate the carboxylate shift process usually observed in Zn(II) acetate complexes. Also, it is of interest , at least from the educational point of view.

9) The correct word is singlets not signals.

Journal Pre-proof

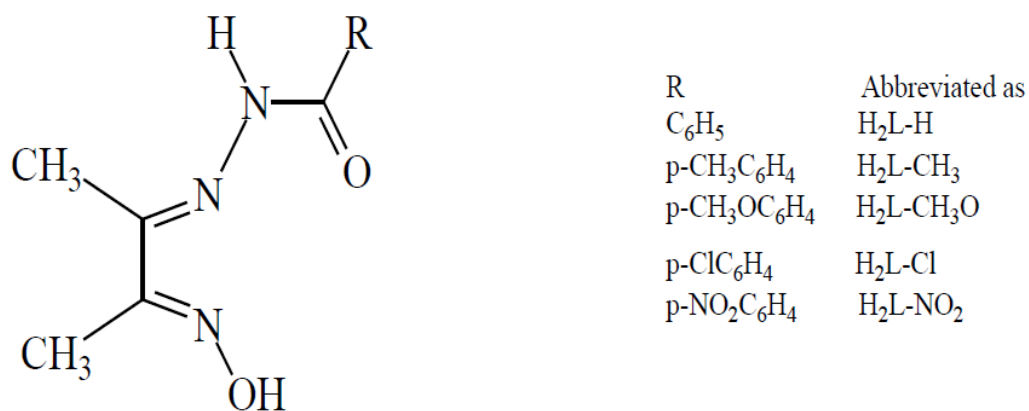
	[Zn(HL-H)(OAc)] <sub>2</sub> .H <sub>2</sub> O (1)	[Zn(HL-CH <sub>3</sub> )(OAc)] <sub>2</sub> .H <sub>2</sub> O (2)	[Zn(HL-Cl)(OAc)(H <sub>2</sub> O)].2H <sub>2</sub> O (4)	[Zn(HL-NO <sub>2</sub> )(OAc)] <sub>n</sub> (5)
Empirical formula	C <sub>26</sub> H <sub>32</sub> N <sub>6</sub> O <sub>9</sub> Zn <sub>2</sub>	C <sub>28</sub> H <sub>36</sub> N <sub>6</sub> O <sub>9</sub> Zn <sub>2</sub>	C <sub>13</sub> H <sub>20</sub> ClN <sub>3</sub> O <sub>7</sub> Zn	C <sub>13</sub> H <sub>14</sub> N <sub>4</sub> O <sub>6</sub> Zn
Formula weight	703.32	731.37	431.14	387.65
Temperature (K)	293(2)	299(2)	293(2)	293(2)
Wavelength (Å)	0.71073	1.54180	0.71073	0.71073
Crystal system	Monoclinic	Monoclinic	Triclinic	Monoclinic
Space group	P2 <sub>1</sub> /c	P2 <sub>1</sub> /c	P-1	P2 <sub>1</sub> /c
Unit cell dimensions				
a (Å)	15.890(2)	12.962(2)	7.704(1)	8.206(1)
b (Å)	10.639(2)	18.580(3)	9.159(1)	6.6160(8)
c (Å)	17.963(3)	13.780(2)	13.198(2)	14.865(2)
α (°)	90	90	95.46(1)	90
β (°)	93.12(2)	98.02(2)	100.70(2)	103.03(1)
γ (°)	90	90	95.52(2)	90
Volume (Å <sup>3</sup> )	3032.2(9)	3286.2(9)	904.7(2)	786.25(17)
Z	4	4	2	2
Calculated density (Mg/m <sup>3</sup> )	1.541	1.478	1.583	1.637
Absorption coefficient (mm <sup>-1</sup> )	1.642	2.300	1.544	1.600
F(000)	1448	1512	444	396
Crystal size (mm)	0.10x0.08x0.01	0.55x0.55x0.50	0.24x0.14x0.08	0.40 x 0.12 x 0.02
θ range for data collection(°)	2.54 to 26.37	3.44 to 66.99	2.60 to 26.37	2.55 to 26.37
Limiting indices	-19<=h<=17, -12<=k<=13, -11<=l<=22	-15<=h<=13, -22<=k<=26, -16<=l<=16	-9<=h<=7, -10<=k<=11, -15<=l<=16	-10<=h<=7, -8<=k<=6, -18<=l<=18
Reflections collected /unique	12101/6064[R(int) = 0.2502]	11089/5854[R(int) = 0.0562]	6473/3692[R(int) = 0.0206]	3046 / 2334 [R(int) = 0.0206]
Completeness to θ	26.37 97.9%	66.99 99.9%	26.37 99.5%	26.37 99.7%
Max. and min. transmission	0.9838 and 0.8530	0.3168 and 0.2940	0.8864 and 0.7082	0.9687 and 0.5669
Absorption correction	Semi-empirical from equivalents	Psi-scan	Semi-empirical from equivalents	Semi-empirical from equivalents
Refinement method	Full-matrix least-squares on F <sup>2</sup>	Full-matrix least-squares on F <sup>2</sup>	Full-matrix least-squares on F <sup>2</sup>	Full-matrix least-squares on F <sup>2</sup>
Data/restraints/parameters	6064/68/394	5854/0/427	3692/7/250	2334 / 1 / 222
Goodness-of-fit on F <sup>2</sup>	0.660	1.144	1.092	1.060
Final R indices [I>2σ(I)]	R1 = 0.0782, wR2 = 0.0531	R1=0.0359, wR2=0.0920	R1=0.0453, wR2=0.0956	R1 = 0.0329, wR2 = 0.0760
R indices (all data)	R1 = 0.3980, wR2 = 0.0966	R1=0.0389, wR2=0.0934	R1=0.0672, wR2=0.1068	R1 = 0.0402, wR2 = 0.0799

**Table 1:**

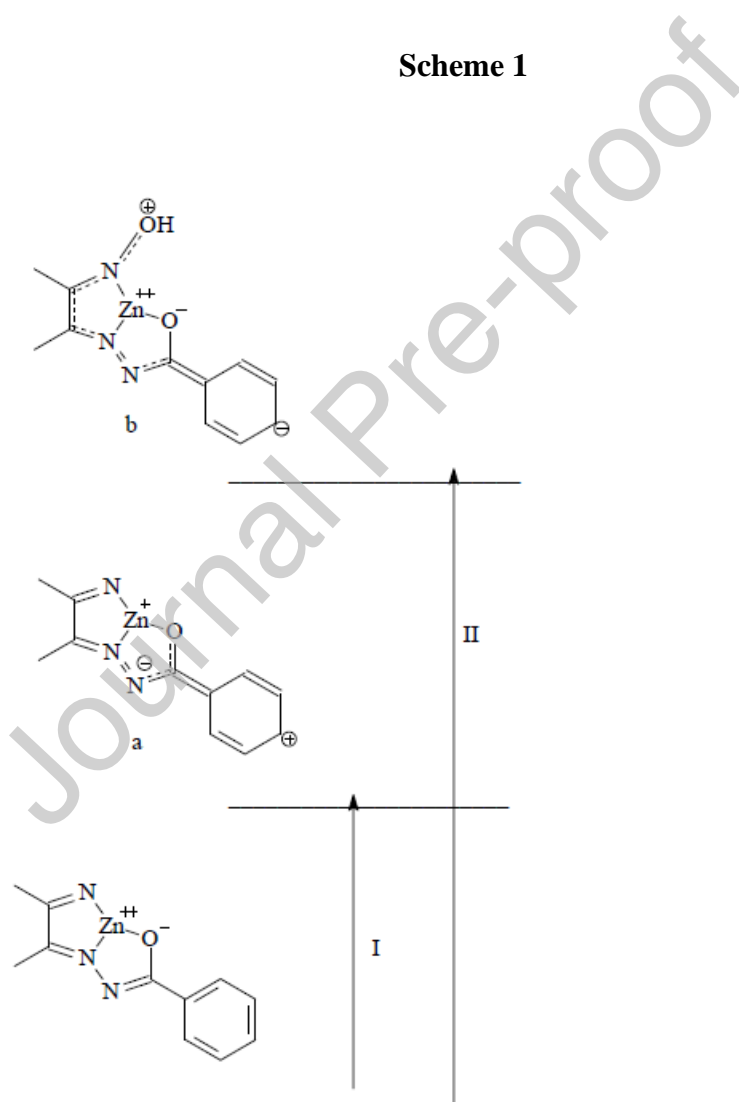
Crystal data and structure refinement parameters for [Zn(HL-H)(OAc)]<sub>2</sub>.H<sub>2</sub>O **1**, [Zn(HL-CH<sub>3</sub>)(OAc)]<sub>2</sub>.H<sub>2</sub>O **2**, [Zn(HL-Cl)(OAc)(H<sub>2</sub>O)].2H<sub>2</sub>O **4** and [Zn(HL-NO<sub>2</sub>)(OAc)]<sub>3</sub> **5**.

Complex	$\alpha (^{\circ})$	$\beta (^{\circ})$	$\tau$
<b>1</b> , Zn1 Zn2	N1 – Zn1 – O1 = 135.5	N3 – Zn1 – O2 = 151.8	0.272
	N4 – Zn2 – O1 = 147.2	N6 – Zn2 – O6 = 149.8	0.043
<b>2</b> , Zn1 Zn2	N2 – Zn1 – O3 = 146.0	N1 – Zn1 – O1 = 149.7	0.062
	N5 – Zn2 – O3 = 139.2	N4 – Zn2 – O6 = 150.0	0.180
<b>4</b> , Zn1	N2 – Zn1 – O2 = 139.8	N3 – Zn1 – O1 = 149.4	0.160
<b>5</b> , Zn1	N2 – Zn1 – O2 = 135.4	N1 – Zn1 – O1 = 148.0	0.210

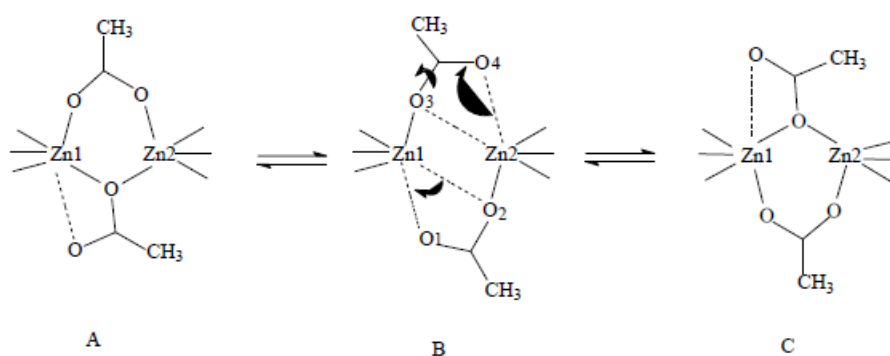
**Table 2:** Tetragonality parameters ( $\tau$ ) calculated for **1**, **2**, **4** and **5** Zn(II) acetate complexes



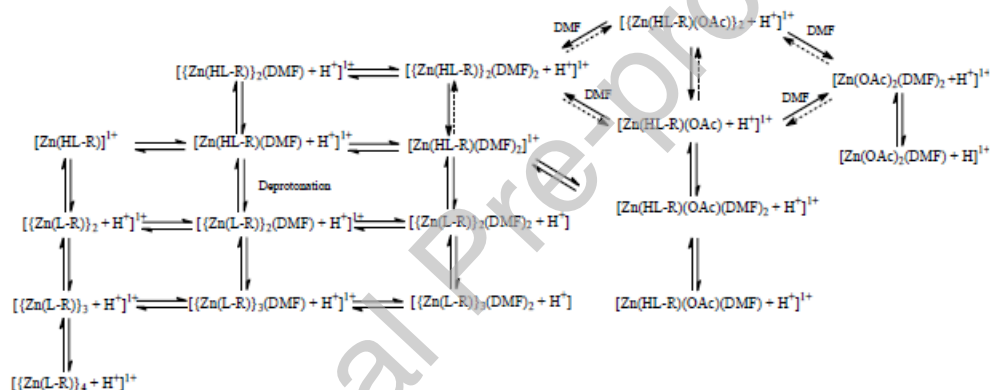
Scheme 1



**Scheme 2:** Excited states involved in the absorption spectra of Zinc(II) acetate complexes (1–5).



**Scheme 3:** Interconversion between syn – syn bidentate bridging acetate and monoatomic bridging acetate in (1 – 3)



**Scheme 4:** Equilibria between different ionic species generated, in DMF/MeOH, for (+)ESI MS spectra of 1 – 5 complexes. Only DMF solvated ionic species are given.

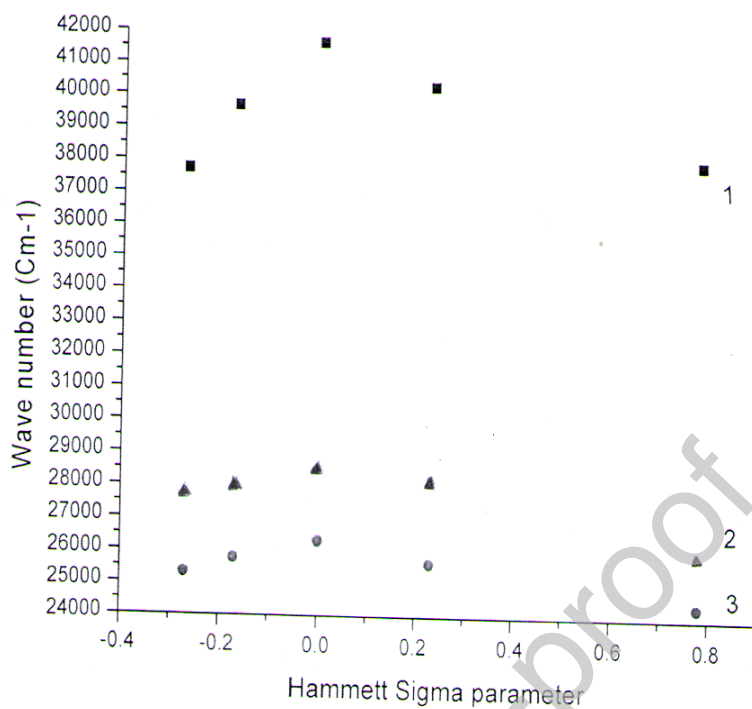


**Figure 1:** Plots of band energies ( $\text{Cm}^{-1}$ ) of  $\pi - \pi^*$  transitions (1, 2) and MLCT transitions (3) against Hammett sigma parameter for 1 – 5 complexes.

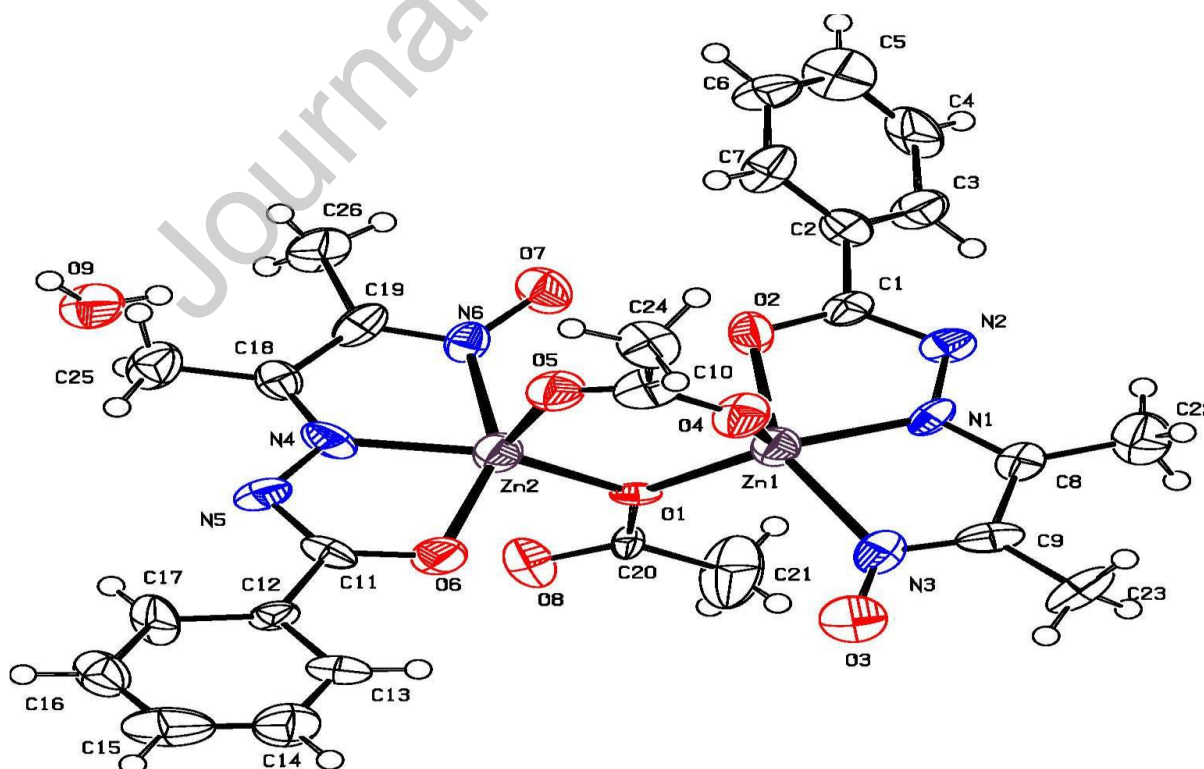


**Figure 2:** Molecular structure of  $[\{Zn(HL-H)(OAc)\}_2] \cdot H_2O$  (**1**) at the 50% probability level.

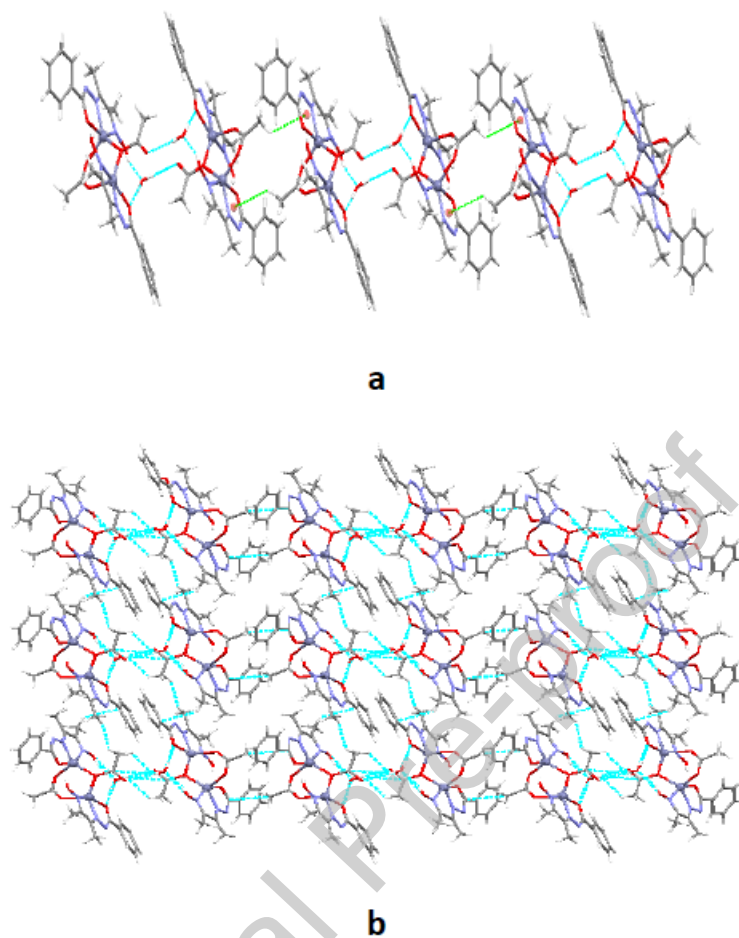


**Figure 3:** a) 1-D chain of hydrogen bonded tetranuclear units of (**1**) along *a*-axis (a-chain) and b) 2-D layer of a-chains extended parallel to *ac*- plane.

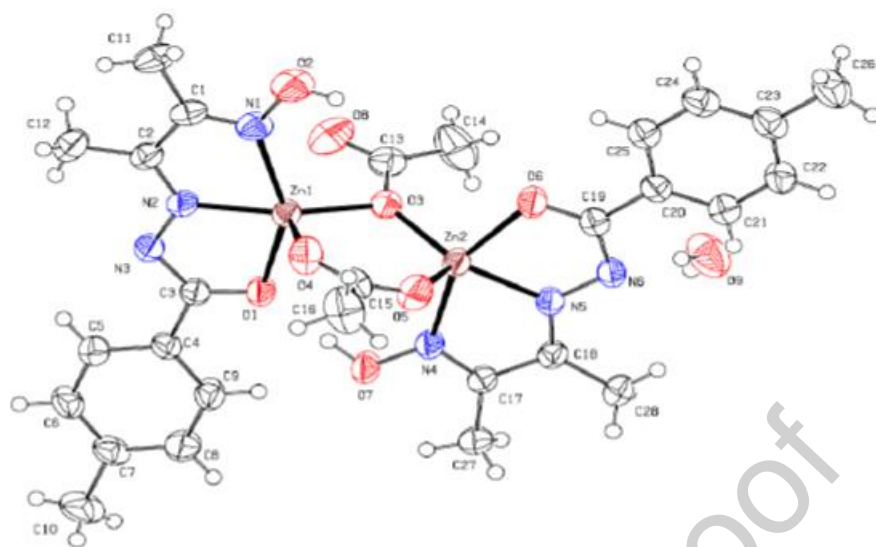


**Figure 4:** Molecular structure of  $[\{Zn(HL-CH_3)(OAc)\}_2] \cdot H_2O$  (**2**) at the 50% probability level.

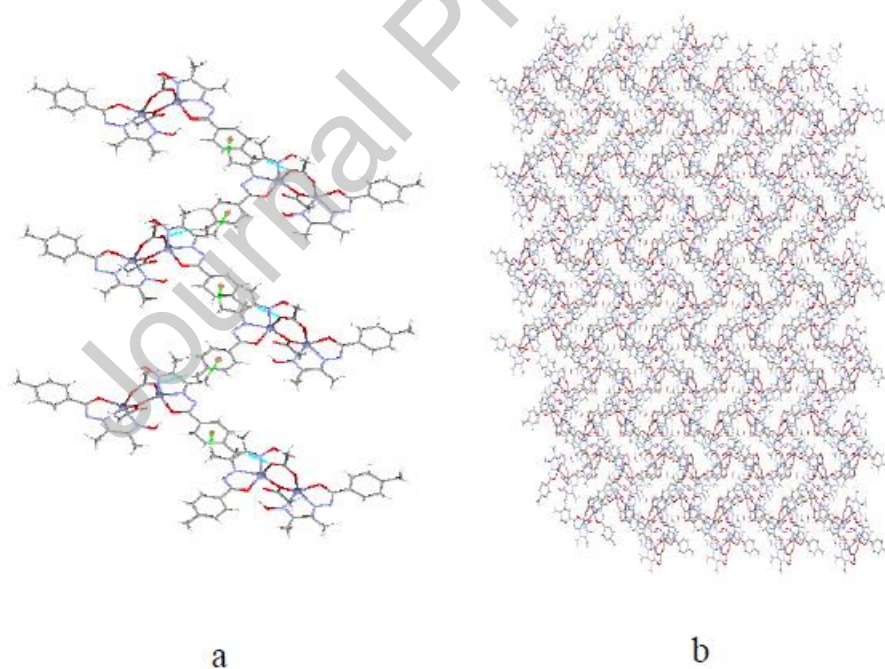


**Figure 5:** 1-D helical chain of the dinuclear molecular units along  $c$ -axis (**a**) and 2-D layer of helical chains extended parallel to  $bc$ -plane (**b**).

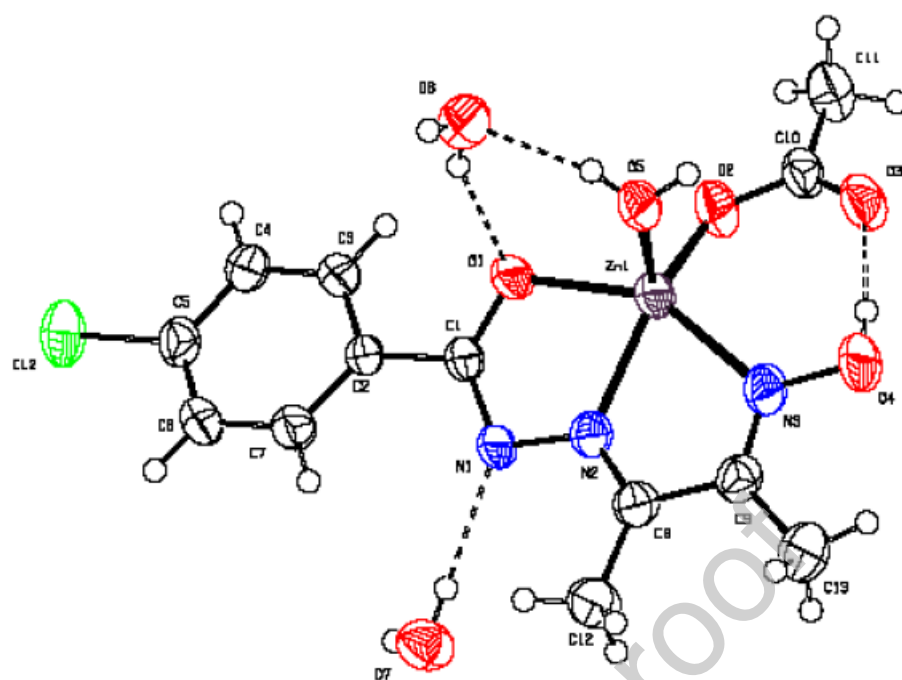
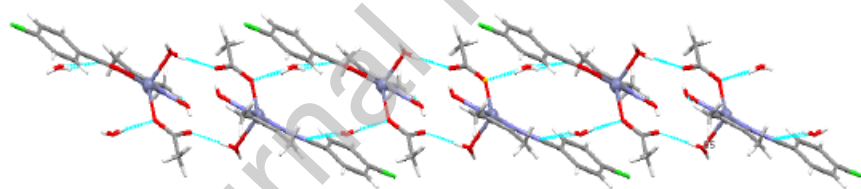
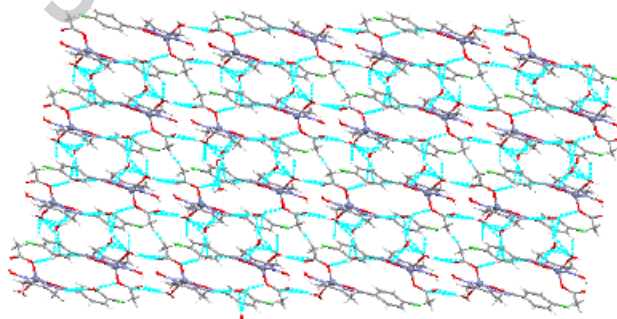


Figure 6

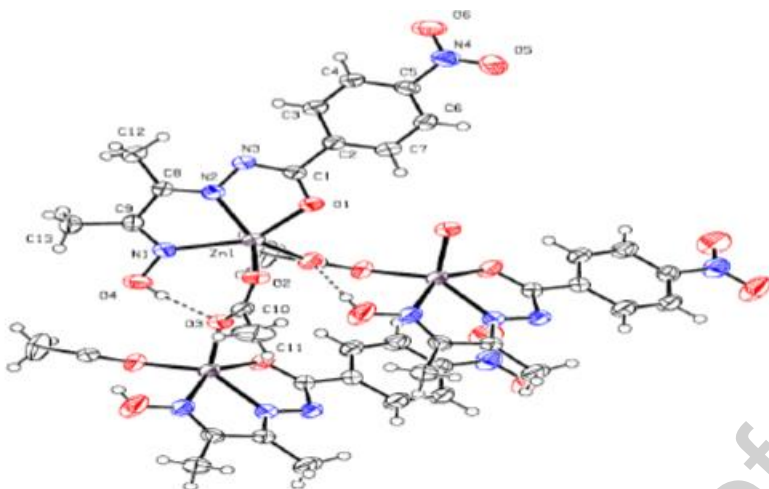


a

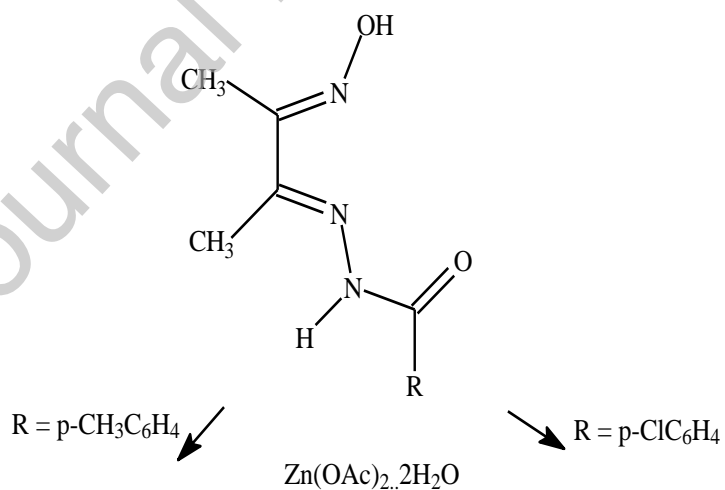


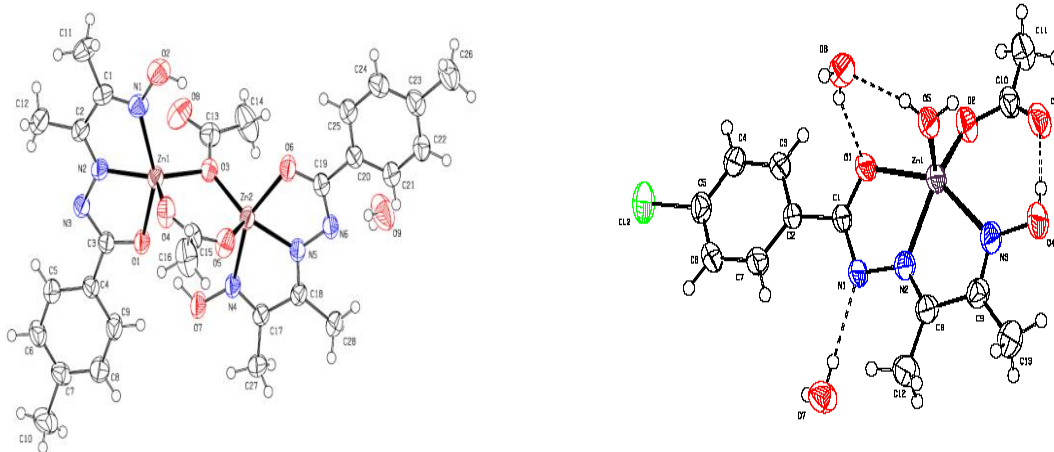
b

**Figure 7:** 1-D chain of head to tail hydrogen bonded dimeric units of **4** along *c*-axis (**a**) and 2-D layer of the dimeric units extended parallel to *ac*-plane (**b**).



**Figure 8:** Molecular structure of trimolecular unit of  $[\{Zn(HL-NO_2)(OAc)\}_3]_n$  (**5**) at the 50% probability level.





Graphical Abstract

Journal Pre-proof